Materials Today Chemistry 56 (2026) 103905

Contents lists available at ScienceDirect

Materials Today Chemistry

journal homepage: www.journals.elsevier.com/materials-today-chemistry/

Advances in gas sensing technologies for harsh environments

Kewei Liu [a], Yiwen Zhou [b,c], Yongbin Qin [d], Carla Bittencourt [b], Zichen Zheng [b,*]

[a] School of Public Health, Shanghai Jiao Tong University School of Medicine, Shanghai, 201203, China
[b] Chimie des Interactions Plasma-Surface (ChIPS), Research Institute in Materials Science and Engineering, University of Mons, Av. Nicolas Copernic 3, Mons, 7000, Belgium
[c] College of Mechanical Engineering, Yangzhou University, Yangzhou, 225127, China
[d] Faculty of Engineering, Kyushu Institute of Technology, 1-1 Sensui-cho, Tobata-ku, Kitakyushu, Fukuoka, 804-8550, Japan

ARTICLE INFO

Keywords:
Gas sensor
High temperature
High humidity
Low temperature
Vacuum

ABSTRACT

The transition toward net-zero emissions and the development of extreme-service machinery have created a growing demand for robust gas-sensing technologies capable of reliable operation in harsh environments. Gas-sensing research is therefore moving beyond laboratory-scale performance optimization toward sensors designed for well-defined extreme-service conditions. Integrating interdisciplinary insights from materials engineering, solid-state physics, and environmental science, this review focuses on research conducted over the past five years. It adopts an environment-driven framework that connects external stressors with sensing mechanisms, performance degradation, and engineering countermeasures. Current gas-sensing technologies are critically assessed in terms of adsorption-desorption behavior, surface reactions, charge or ion transport, mass transfer, and device stability with application-specific design requirements in aerospace, deep-sea exploration, geothermal engineering, combustion or exhaust monitoring, and planetary investigation. Finally, emerging challenges in material durability, packaging reliability, calibration stability, system integration, and domain-adaptive modeling are identified, guiding the development of reliable gas-sensing platforms for continuous extreme-environment monitoring and future frontier technologies.

1. Introduction

In recent years, there has been a marked increase in the demand for reliable sensor systems capable of sustained operation under extreme service conditions, such as those encountered in geothermal drilling, turbine operation, and planetary space exploration. Harsh environments present major challenges for gas detection. For instance, in situ trace-gas measurements at the Venusian surface occur in a sulfur-rich atmosphere at ~460°C and at pressures ~90 times Earth's surface pressure [1]. Accurate measurement of oxygen concentration in oxy-fuel combustor exhaust streams requires sensors capable of withstanding temperatures approaching 1000°C [2]. In the context of deep-sea extreme-environment monitoring, in situ quantification of dissolved CH_4, CO_2, and H_2S in hydrothermal vent fluids demands sensors tolerant of ~450°C and strongly acidic conditions (pH < 3) [3,4]. These applications demand high robustness of sensors against extreme temperatures, pressures, and mechanical stresses, leading to the development of integrated solutions in sensing elements, electronics, and packaging technologies [5].

This gap motivates a review that connects laboratory-level sensing studies to field-relevant harsh-environment requirements. As illustrated in Fig. 1, research on gas detection in harsh environments has steadily increased over the past 20 years. Notably, many studies simulate local extremes in the laboratory, such as heating the sensor element, humidifying the inlet stream, or pressurizing a sealed chamber, rather than operating under truly harsh ambient conditions, thereby creating a gap relative to real-world applications. This review focuses on gas-sensing technologies for extreme environments, including thermal extremes, moisture-laden atmospheres, pressurized systems, low-pressure rarefied gases, and near-vacuum conditions. However, research under authentic coupled harsh environments remains limited.

For primary sensor architectures, gas sensors convert interactions between gaseous species and solid or liquid matrices into measurable electrical or optical signals [6,7]. The combination of high sensitivity, rapid response, low cost, and simple integration has kept this field a major research focus. Gas sensing technology plays a critical role across various sectors, including environmental monitoring [8,9], industrial safety [10,11], medical diagnosis [12,13], agricultural storage [14,15], and aerospace exploration [16,17]. Gas-sensing performance supports

* Corresponding author. Chimie des Interactions Plasma-Surface, University of Mons, Av. Nicolas Copernic 3, Mons, 7000, Belgium.
E-mail address: Zichen.ZHENG@umons.ac.be (Z. Zheng).

https://doi.org/10.1016/j.mtchem.2026.103905
Received 25 May 2026; Received in revised form 15 July 2026; Accepted 1 August 2026
Available online 4 August 2026

vital infrastructure and strategic capabilities. Additionally, integrating gas sensors with the Internet of Things (IoT) and artificial intelligence (AI) has enabled remote monitoring and smart data processing, expanding their uses [18]. From a market standpoint, the global gas sensor industry is rapidly expanding. According to a Grand View Research report, the worldwide gas sensor market was valued at USD 2.90 billion in 2023 and is expected to grow at a compound annual growth rate (CAGR) of 9.5% from 2023 to 2030 [19]. This growth is driven by increased deployment across sectors like manufacturing, healthcare, and agriculture, where gas sensors improve efficiency, safety, and regulatory compliance [20].

Despite this widespread deployment, most existing gas sensors are optimized for mild ambient conditions. Exposure to extreme temperatures, high humidity, or vacuum conditions often degrades sensing materials, device structures, and signal stability, which lowers measurement reliability [21–24]. While moderate heating can enhance gas-sensing performance, excessively high temperatures can be harmful [25]. At high temperatures, adsorbed gas molecules become too mobile and desorb too quickly from the surface, preventing participation in sensing reactions [26]. Water molecules competing for adsorption and capillary condensation within mesoporous structures in high-humidity environments can change surface reaction kinetics and obscure the target gas signals [27]. Vacuum or very low temperatures may cause active sites in the sensing material to fail [28]. These issues make gas detection in extreme environments a critical challenge in global sensing.

Extreme-temperature environments are common in operational scenarios. For high-temperature conditions, such as monitoring internal combustion engine exhaust and controlling metallurgical processes, sensing materials must display excellent thermal stability and resistance to sintering. In ultra-low temperature conditions, like liquefied hydrogen and liquefied natural gas storage and transfer (−253°C and −162°C) [29], as well as thermal-vacuum space applications with large thermal swings (from −120°C to +120°C), sensor design must address issues such as carrier freeze-out, slowed adsorption-desorption kinetics, condensation, and thermal mismatch stresses. High-temperature sensing is well covered in the existing literature, while low-temperature and cryogenic sensing are emerging topics driven by specific applications. Studies have shown that pure SnO_2 nanowires showed a 5.95 response to 10 ppm H_2 gas at 300°C, which decreased slightly to 4.85 at 350°C, indicating poor high-temperature response stability. However, nanowires coated with an Al_2O_3 layer (optimal thickness of 4.5 nm) using atomic layer deposition (ALD) increased the sensor's response at 350°C to 152.54, more than 30 times that of the uncoated sample. Even at higher temperatures such as 400°C and 450°C, the sensor maintained high responses of 57.32 and 12.76, respectively, demonstrating good high-temperature performance. Therefore, the Al_2O_3 shell helps suppress grain coarsening and electron dissipation, while enhancing thermal stability and gas sensing by modulating the interface barrier and forming a SnO_2-Al_2O_3 heterojunction. Additionally, the core-shell structure showed excellent selectivity, repeatability, and long-term stability, making it a reliable solution for hydrogen leakage detection in high-temperature environments [30]. Therefore, maintaining measurement accuracy across temperature extremes remains a key challenge in harsh-environment gas sensing. High-temperature gas sensing strategies include using sintering-resistant oxide sensing layers produced via nanoparticle exsolution, refractory packaging, and wide-bandgap SiC--based sensors and electronics validated at $\geq$ 500°C [31,32]. Low- and cryogenic-temperature gas sensor operation can rely on local micro-heating or photoactivation to restore surface kinetics, combined with fiber-optic systems for *in situ* detection [33]. Complementary measures involve physics-informed temperature compensation and data-driven drift correction.

Humidity is a crucial environmental factor affecting the performance of gas sensors. Under high or low humidity conditions, key metrics such as sensitivity, selectivity, and response/recovery times (t_{res}/t_{rec}) are often notably impacted. Extreme humidity levels are encountered across many operational scenarios. In high-humidity environments, such as wastewater treatment and wet flue-gas scrubbing, sensing materials should demonstrate hydrophobicity and resistance to capillary condensation to maintain selectivity and stability. In ultra-low-humidity environments (less than 5%), some materials such as doped polymers, conductive polymers, and carbon-based composites, may lose proton conduction or interface charge balance, resulting in drift or reduced sensitivity [34]. In metal-oxide-semiconductor (MOS) gas sensors, high humidity can suppress the redox reactions of target gases, significantly reducing detection sensitivity. In certain polymer-based or polymer-nanocomposite sensors, humidity can cause material swelling, alter conductivity, and lead to signal drift and measurement errors [35,36]. Moreover, humidity significantly affects the performance of optical gas sensors by altering the refractive index and volume of the sensing film upon moisture absorption, leading to spectral shifts and gas detection errors. Condensed water films on the sensing surface also disrupt light transmission, further impacting measurement accuracy [37,38]. Humidity compensation is therefore central to reliable

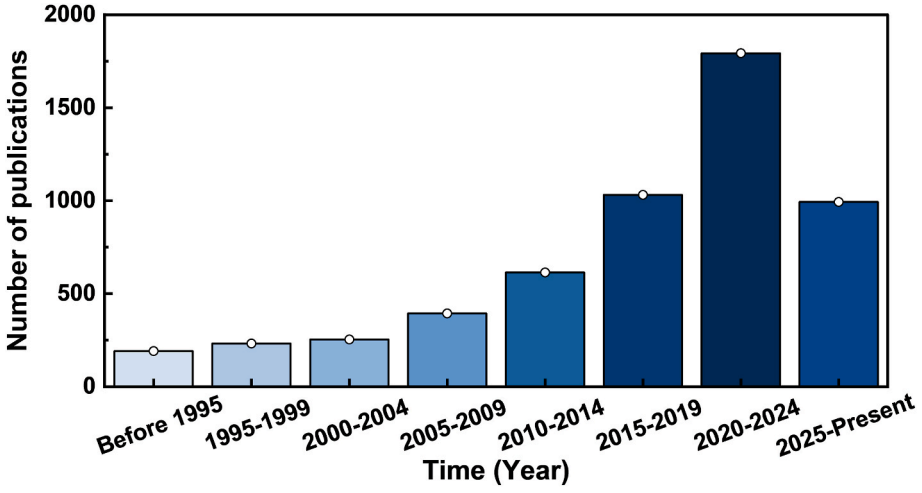

Fig. 1. Annual number of publications on harsh-environment gas sensing retrieved from the Scopus database using the TITLE-ABS-KEY((“gas sensor*” OR “gas sensing” OR “gas detection” OR “gas monitor*”) AND (“harsh environment*” OR “extreme environment*” OR “high temperature” OR “low temperature” OR cryogenic OR “high humidity” OR vacuum OR “corrosive environment*” OR “high pressure”)) AND (DOCTYPE(ar) OR DOCTYPE(re)). Articles and reviews published from database inception to the retrieval date were included. The asterisk (*) denotes a Scopus wildcard used to capture word variants.

operation in moisture-rich environments. Current approaches include hydrophobic coating materials, environmental self-calibration algorithms, and multi-parameter joint-detection strategies.

Pressure extremes are common in various sensing environments, altering gas density, adsorption flux and surface reaction equilibria. At high pressures, such as in deep wells or turbine combustors, sensing materials require high structural rigidity and stable adsorption capacity to prevent pore collapse and signal saturation, thereby ensuring consistent gas-solid interactions. At ultra-low pressures nearing vacuum, such as in aerospace or vacuum systems, materials should have defect-rich active sites and large surface areas to capture trace molecules. Meanwhile, assisted activation methods, such as local heating or photoexcitation, help maintain detection sensitivity. Operating in a vacuum or near-vacuum can reduce background interference and enhance signal-to-noise ratio, but it also presents several challenges. Under low-pressure conditions, fewer molecular collisions slow diffusion, potentially affecting the sensor t_{res}. Additionally, sensor sensitivity may decrease in the absence of oxygen or under abnormal pressure conditions, especially for sensors that rely on redox reactions or an air background, such as metal oxide or electrochemical gas sensors. Furthermore, the target gas concentration in a vacuum can be easily affected by adsorption, leakage, or system inaccuracies, leading to increased measurement errors [22,39]. Therefore, extreme pressures influence adsorption and surface reaction kinetics, thereby shaping gas-sensing signals. Under high pressure, sensing layers must maintain their structural integrity and adhere strongly to the substrate. They should utilize accessible meso- to macro-porous networks that are resistant to compaction to prevent site saturation and to control defect and catalytic site density. At ultra-low pressures near vacuum, when chemiresistive contrast is insufficient, optical methods (e.g., tunable diode laser absorption spectroscopy or cavity-enhanced techniques), resonant mass sensors (e.g., quartz crystal microbalance (QCM) or surface acoustic wave sensors), or field-emission readouts can be used to restore sensitivity.

Beyond temperature, humidity, and pressure, harsh-environment gas sensing also includes corrosive, dusty, high-flow, high-radiation, and explosive atmospheres, each requiring specialized materials and structural designs to ensure stability, selectivity, and safety. However, laboratory tests can sometimes be unreliable, as previous comparisons of dissolved CH_4 measured in fluids collected by conventional versus gas-tight sampling have shown [40]. Therefore, in situ detection that maintains native conditions has become a preferred method for monitoring extreme environments. Most importantly, gas sensors designed for harsh environments are becoming increasingly vital for maintaining safety and operational efficiency across various industries. These sensors are built to operate reliably in tough conditions. Industries such as petrochemicals, mining, aerospace, and defense use these sensors to detect toxic, hazardous, or flammable gases, helping prevent accidents and protect personnel. Advances in technology are driving gas sensor development toward higher sensitivity, shorter t_{res}, lower power consumption, and smarter features. The use of new materials, such as nanomaterials and thin-film technologies, along with advanced manufacturing techniques, has greatly improved sensor stability and reliability under extreme conditions. These trends motivate a mechanism-oriented review of gas-sensing technologies for harsh environments.

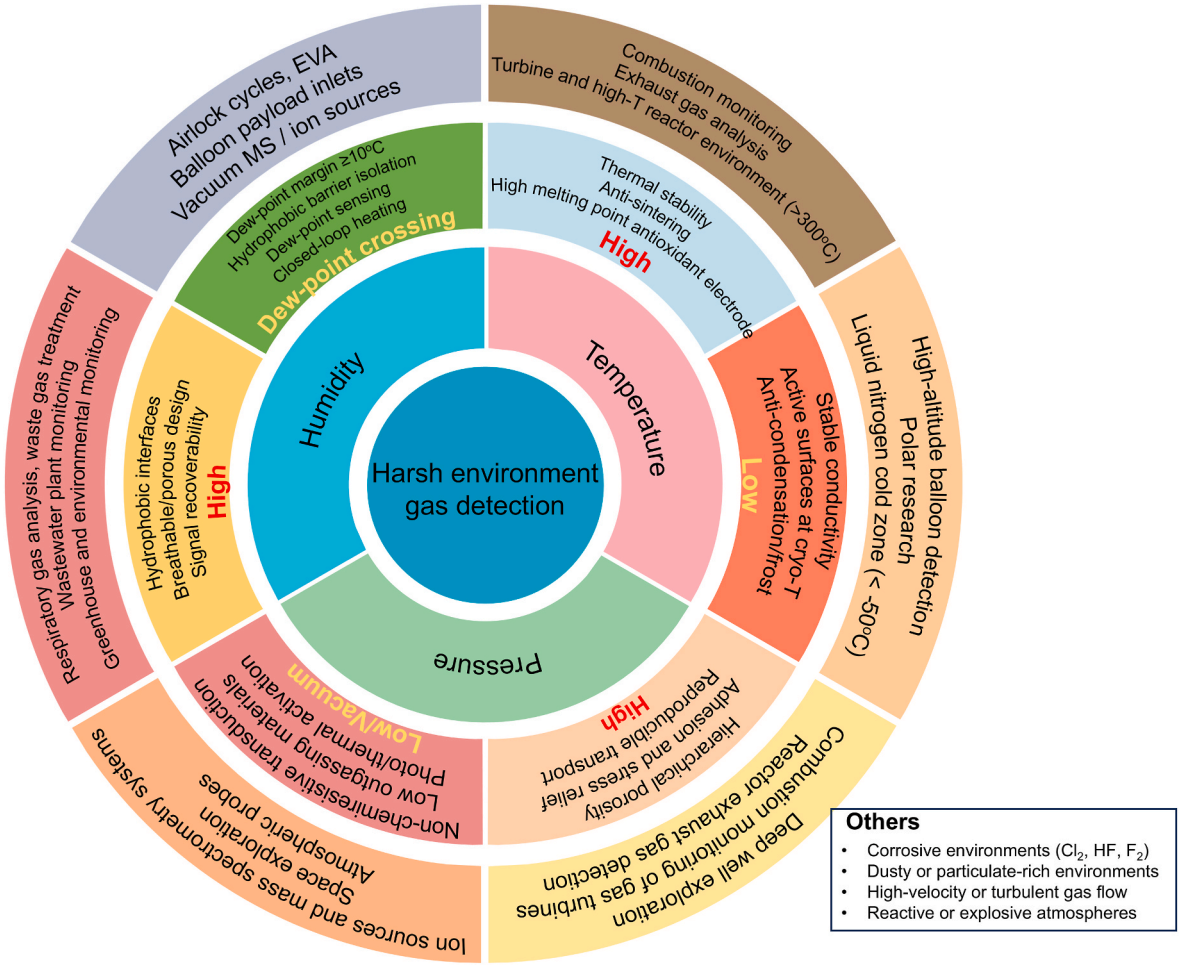

Fig. 2. Illustrative diagram of the characteristics and specific applications of gas detection in different harsh environments.

In this review, advancements in gas-sensing technologies designed for extreme environments over the past five years are categorized and compared. The characteristics and specific applications of gas detection in various harsh settings are illustrated in Fig. 2. We begin by introducing the fundamental sensing principles and material considerations essential for sensor performance under challenging conditions. Next, we examine specific environmental challenges, including high and low temperatures, high humidity, and vacuum, analyzing how different sensing materials and device architectures respond to these stressors. By reviewing key research efforts and identifying common limitations and solutions, we highlight emerging strategies to improve sensor resilience and reliability. Additionally, we explore representative application fields where these technologies are being used or envisioned, providing insights into their practical implications. Through this comprehensive analysis, we aim to provide a valuable resource for researchers and engineers, guiding the development of next-generation gas sensors capable of withstanding extreme operating conditions. Notably, in this review, "harsh environment" and "extreme environment" are used interchangeably to describe non-standard operating conditions that can compromise gas-sensing performance.

2. Common gas detection techniques

In extreme environments, gas detection can rely on various transduction mechanisms, including chemiresistive, solid-electrolyte/electrochemical, optical, acoustic/resonant, ionization, and mass spectrometric methods, each balancing stability, selectivity, and sensitivity under non-standard temperature, humidity, and pressure conditions. In such scenarios, overall performance is determined not only by the sensing material but also by controlled gas delivery and reference channels, rigorous calibration and uncertainty analysis, and predictive models that couple adsorption-reaction kinetics with mass transport. Additionally, data-driven signal compensation and multi-sensor integration approaches can improve reliability when responses from individual sensors are limited. Therefore, the selection of a sensing technology should be guided by the target gas, operating conditions, power budget, calibration stability, and system-level integration complexity.

2.1. Chemoresistive gas sensing

In chemiresistive sensors, target gases interact with the sensing layer, altering its conductivity. The sensing response generally involves gas molecule diffusion, surface or interfacial reactions, and charge-carrier transport within the solid. When gas molecules reach the semiconductor sensing surface, interfacial charge-transfer processes are initiated through surface states, catalytic sites, or defect-mediated pathways. In air, ambient O_2 can adsorb and withdraw electrons to form ionic oxygen species, such as O_2^-, O^-, or O^{2-}. This charge redistribution causes surface band bending and creates an interfacial potential barrier, forming a space-charge region that modulates the material's conductivity, with electron depletion in n-type semiconductors and hole accumulation in p-type, as shown in Fig. 3a and b [43]. For n-type semiconductors, reducing gases consume pre-adsorbed oxygen species, lowering the surface barrier and decreasing resistance. P-type materials show opposite behavior. Resistance increases in reducing environments and decreases in oxidizing environments. The response amplitude correlates with analyte concentration; thus, concentration can be estimated from changes in resistance relative to the baseline, as shown in Fig. 3c.

In addition, morphology-tailored MOS-carbon nanoarchitectures and metal-organic framework (MOF)-derived metal oxides represent two complementary design strategies for chemiresistive gas sensors [44, 45]. The former balances reactive oxide domains with conductive carbon networks to enhance resistance modulation and molecular discrimination, whereas the latter uses precursor-guided conversion to regulate porosity, morphology, and active oxide sites for gas-dependent selectivity. Furthermore, heteroatom-induced bonding regulation in metal oxides can modify the crystal structure and surface reactivity, providing another route to optimize active-site chemistry and gas-sensing performance [46]. Collectively, heterostructure construction, heteroatom doping, and defect engineering provide effective routes to modulate charge transport, surface reactivity, and active-site availability in chemiresistive gas sensors, thereby enhancing response stability, sensitivity, and selectivity under extreme conditions (Fig. 3d) [47–49].

Nanocomposite engineering offers another important strategy for improving chemical and gas-sensing performance by integrating gas-reactive components with conductive, polymeric, piezoelectric, or textile-supported matrices. These hybrid structures can increase the

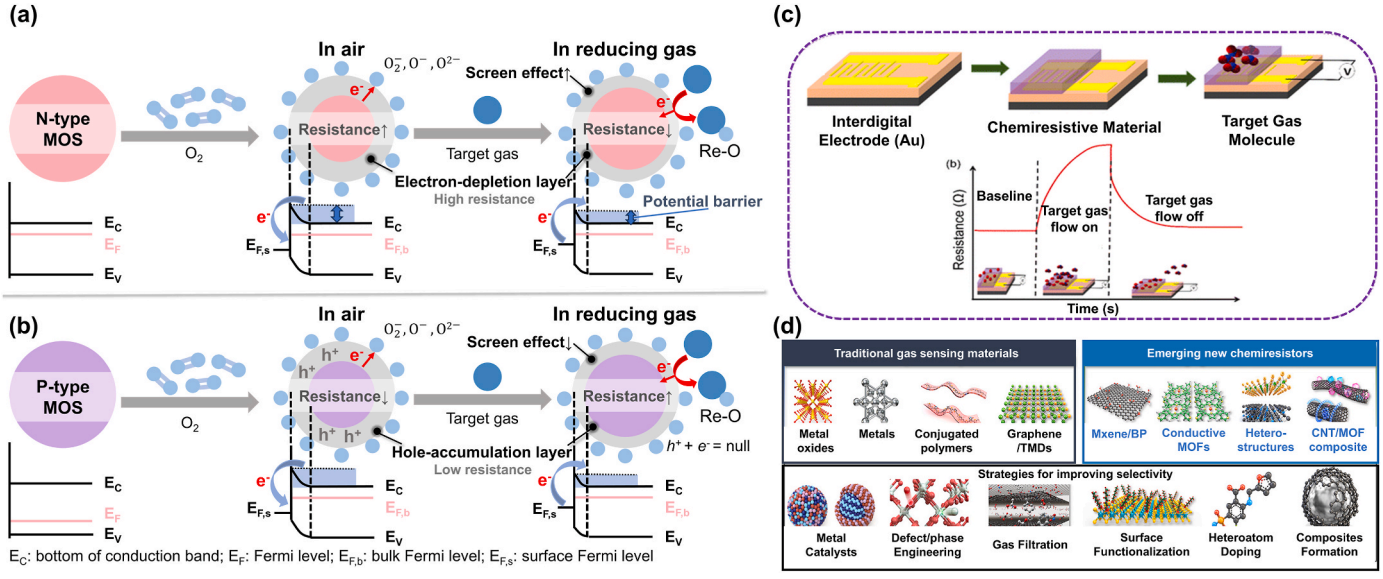

Fig. 3. Schematic of the sensing mechanism for (a) n-type and (b) p-type MOS semiconductor toward reducing gases. (c) Schematic for the chemiresistive sensing mechanism. Reproduced from Ref. [41], Royal Society of Chemistry, open access under CC BY license. (d) Schematic showing materials evolution for chemiresistive sensors and strategies. Reproduced from Ref. [42], American Chemical Society, open access under CC BY license.

number of accessible active sites, regulate interfacial charge transfer, improve structural flexibility, and enhance analyte discrimination through synergistic interactions among phases. For example, polyvinylidene fluoride/TiO_2 nanofiber textiles combine a flexible polymer scaffold with an ethanol-sensitive TiO_2 shell, illustrating the potential of polymer-oxide nanocomposites for flexible, self-powered gas recognition [50]. More broadly, recent studies on piezoelectric and electrochemical composite sensors show that rational phase coupling and interface engineering can expand the material design space for advanced chemical and gas-sensing platforms [51,52].

From an application perspective, chemiresistive sensors are particularly well suited for compact, low-cost, array-based detection because of their simple device structure, broad material tunability, and compatibility with miniaturized electronics [42]. However, deploying them in harsh environments requires careful management of humidity interference, oxygen partial pressure effects, baseline drift, and thermally induced microstructural aging.

2.2. Solid electrolyte gas sensing

Solid-electrolyte sensors based on solid oxide-ion conductors, such as yttria-stabilized zirconia (YSZ), can operate either according to the thermodynamic Nernst relation or Faraday's law. Fig. 4a summarizes the operating principles of these sensors. Mixed-potential gas sensors are solid-electrolyte devices with dissimilar, electrocatalytically active electrodes exposed to the gas phase. The basic setup of mixed-potential sensors is shown in Fig. 4b and c. Multiple redox reactions, including the electrochemical reduction of oxygen and the electrochemical oxidation of the analyte (e.g., combustibles), occur simultaneously at the electrode-electrolyte-gas triple-phase boundary, each with distinct reaction kinetics. As a result, the system electrode does not reach a thermodynamic Nernst equilibrium. Instead, a steady mixed potential is established when the anodic and cathodic partial currents are balanced, and this potential shifts reproducibly with the target gas concentration, as shown in Fig. 4d [53].

Compared with semiconducting chemiresistive sensors, mixed-potential sensors can offer improved selectivity because their signals are governed by electrode-specific electrochemical reaction kinetics rather than non-specific resistance modulation. Selectivity depends on the differing kinetics of specific redox pairs and on adsorption processes that can be tailored through electrode material, composition, and operating temperature. Considerable attention has therefore been directed toward sensing-electrode materials that preserve non-equilibrium gas compositions and avoid premature catalytic equilibration before the gas reaches the electrochemically active interface. Owing to their full solid-state construction, high-temperature operability, and tunable electrode catalysis, mixed-potential sensors have been used for automotive exhaust and industrial flue-gas monitoring. They are being actively explored for hazardous and harsh environments, including combustion control and high-temperature gas analysis [55,56]. Remaining challenges include humidity interference, cross-sensitivity, electrode aging, and reference stability, which require electrode engineering, protective layers, optimized operating temperatures, and signal compensation strategies.

Accordingly, solid-electrolyte sensors are particularly suitable for high-temperature exhaust, combustion, and oxygen- or NO_x-related monitoring, where thermally robust ceramic electrolytes and electrochemical transduction are advantageous [54]. However, their broader use in low-temperature, distributed, or ultralow-power sensing networks is constrained by the need for elevated operating temperatures, stable reference-electrode configurations, and reliable long-term sealing in chemically aggressive gas streams [57].

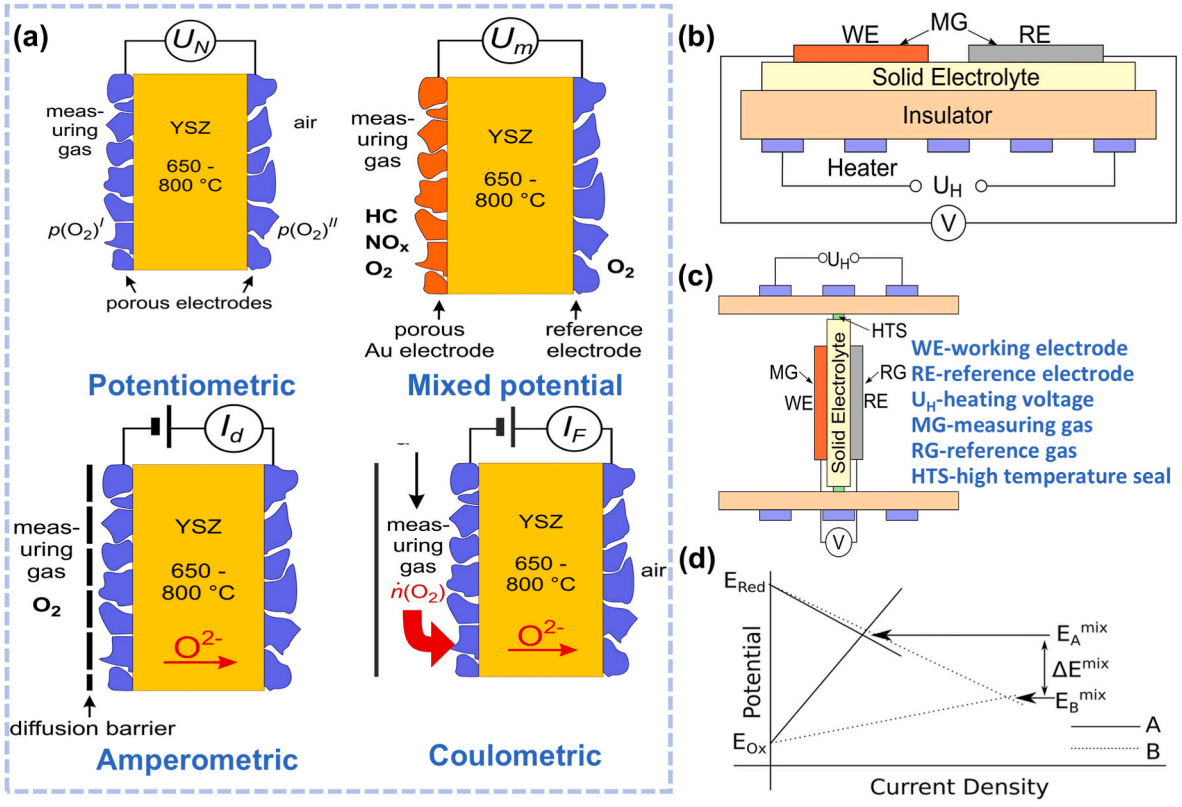

Fig. 4. (a) Basic working principles of solid-electrolyte sensors for oxygen-containing gases of different sensing modes. Basic configurations of mixed-potential sensors: (b) gas-symmetric, (c) with a gas-separated reference electrode. Reproduced from Ref. [53], Copyright© 2023, Elsevier. (d) Current-voltage characteristics of a model sensor with electrodes A and B exhibiting different oxidation/reduction kinetics. The voltmeter records the resulting mixed-potential difference. Reproduced from Ref. [54], Copyright© 2022, Elsevier.

2.3. Optical gas sensing

Optical sensors are widely used for gas detection under extreme conditions because they enable molecule-specific, non-contact, and remote readout. Representative methods include mid-infrared (MIR) sensing, non-dispersive infrared (NDIR) spectroscopy, and surface-enhanced Raman scattering (SERS) [58]. In MIR sensors, fundamental vibrational absorption in the 2-20 μm range is measured using tunable lasers or on-chip waveguides for high selectivity and accurate quantification [59]. In NDIR spectroscopy sensors, both MIR and near-infrared (near-IR) ranges analyze vibrational absorption bands to quantify species [60]. SERS relies on plasmon-enhanced Raman spectra for molecular specificity but requires reproducible substrates and effective preconcentration [61]. Colorimetric sensors convert gas-induced chemical or structural changes into red-green-blue (RGB) imaging or ultraviolet-visible spectroscopy (UV-vis) absorption shifts for simple readout [62]. These methods require careful calibration, interference control, temperature and pressure compensation, miniaturization, and long-term stability.

2.3.1. MIR sensor

The spectral region from 2 to 20 μm, accessible by MIR sensors, overlaps with the fundamental vibrational bands of numerous molecules, enabling highly selective and sensitive measurements. Because it directly probes primary absorption bands, the MIR range supports trace-level quantification with high specificity and reduced spectral interference. Consequently, MIR photonic sensors can provide real-time, non-invasive, and *in situ* analysis, offering rapid and reliable readouts [63]. The MIR region enables concentration-dependent measurements that can be readily quantified using the Beer-Lambert law, which relates absorbance to analyte concentration. MIR is well-suited to extreme conditions because it supports molecule-specific, non-contact, or open-path detection, is insensitive to electromagnetic interference, and can utilize modulation and cavity-based techniques, along with line-shape modeling, to maintain quantitative accuracy under varying temperatures and pressures [64].

2.3.2. NDIR sensor

NDIR measurements also follow the Beer-Lambert relationship. NDIR sensors have been demonstrated to be suitable for multi-gas detection, as illustrated by the detector configuration in Fig. 5a. A key advantage of NDIR over many spectroscopic methods is low power demand, since IR sources in the 1 to 15 μm range can run at lower temperatures, as shown in Fig. 5b. Besides, with minimal maintenance needs, NDIR detectors offer a more economical option than many other systems [65]. However, interference and limit of detection (LoD) remain key limitations, both

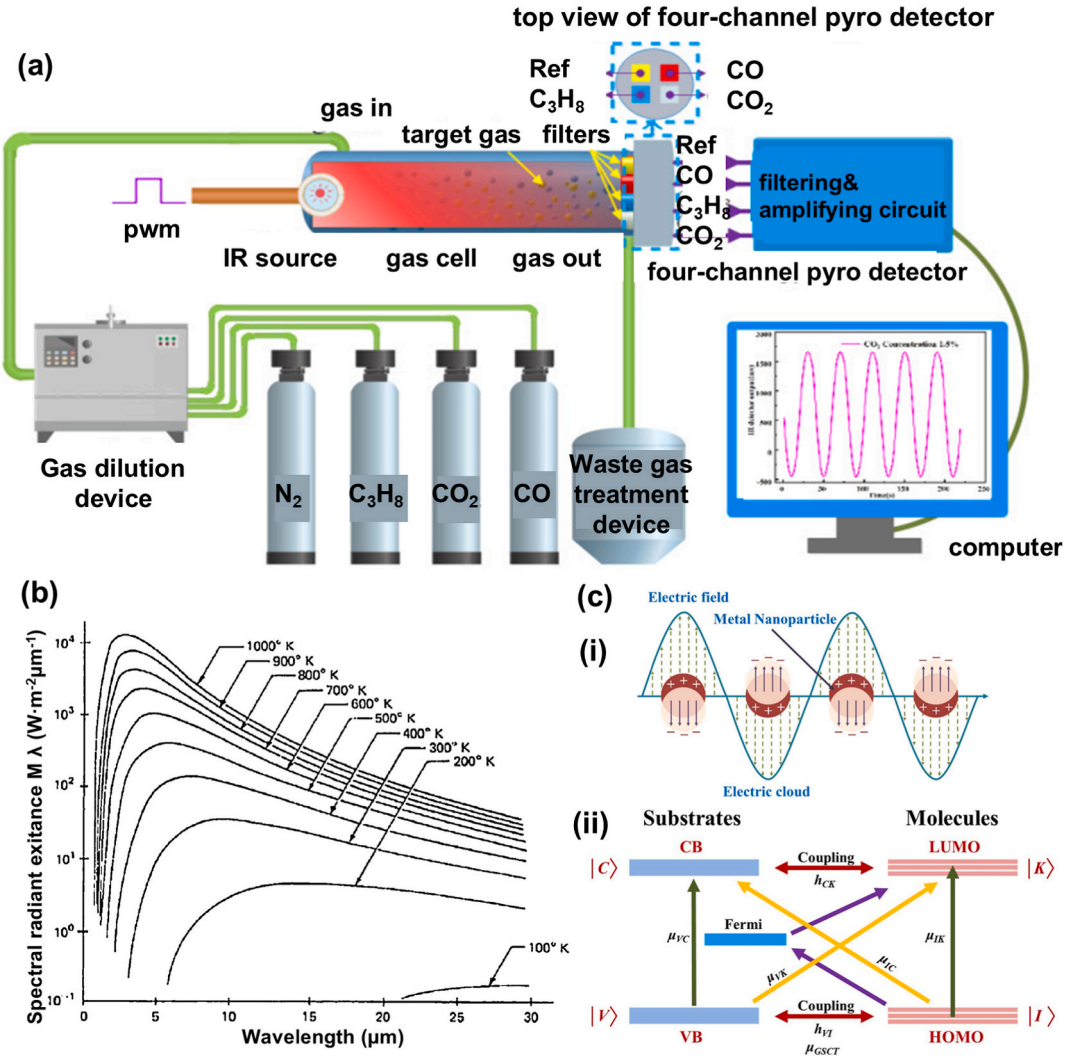

Fig. 5. (a) Layout of the NDIR multi-gas detection system. Reproduced from Ref. [65], MDPI, open access under CC BY license. (b) Blackbody peak wavelength versus temperature, showing a shift to shorter wavelengths at higher temperatures [66], Copyright© 2016, Elsevier. (c) Schematic of SERS spectral enhancement mechanism. Reproduced from Ref. [67]. Copyright© 2024, Elsevier.

governed by the overall signal-to-noise ratio. Interference stems from overlapping absorbers, such as ambient water vapor and carbon dioxide, source or optical background, window contamination, aerosol scattering, and temperature- or pressure-induced baseline drift. Sensitivity is the change in detector output per unit change in the transmitted infrared intensity, whereas LoD is the smallest concentration that can be quantified with a specified level of precision [66]. NDIR sensors are suitable for compact, relatively low-power gas monitoring when the target gas has strong infrared absorption bands. Their robustness stems from filter-based optical configurations, simple optical layouts, and reference-channel designs, but their performance can still be affected by window contamination, spectral overlap, aerosol scattering, and temperature- or pressure-induced baseline drift. Additionally, the NDIR method is limited by its non-specific nature and high LoD (e.g., tens of ppm) [16].

2.3.3. SERS sensor

SERS nanostructures utilize molecule-specific vibrational signatures to generate distinct Raman peaks, enabling the identification of various targets [68]. In SERS, analyte molecules are positioned within the electromagnetic hotspots of plasmonic nanostructures, where enhanced local fields and substrate-adsorbate charge-transfer interactions dramatically amplify the Raman response, allowing sensitive detection of gas-phase species. Electromagnetic enhancement (EM) and chemical enhancement (CM) are the primary mechanisms. When two or more nanoparticles are closely spaced, the nanogap produces strong electromagnetic enhancement, as shown in Fig. 5c(i), whereas CM arises from charge transfer between the substrate and adsorbed molecules (Fig. 5c (ii)). SERS enables sensitive and rapid analysis of complex mixtures. However, its robustness depends on the properties of the nanostructured substrate [61,67]. Compared with absorption-based optical methods, SERS provides localized vibrational fingerprints through plasmonic hotspots and is useful for species with weak infrared absorption. It also allows straightforward silica-fiber delivery to keep electronics outside hazardous areas, supports chemo-selective functionalization and preconcentration for complex humid or corrosive environments, and remains effective for species with weak infrared absorption.

2.3.4. Colorimetric sensor

Colorimetric sensors often capture or preconcentrate analytes within dyes, coordination complexes, polymers, or porous host matrices to enhance selectivity and optical readout. Colorimetric gas sensing translates gas-induced chemical or structural changes into shifts in the visible or UV-vis absorption spectra. In molecular and solid-state chromogenic systems, color changes typically arise from changes in conjugation, chromophore or auxochrome transformation, ligand exchange at metal centers, or solid-state phase transitions. These processes can modify electronic transition energies, d-d or charge-transfer bands, oxidation states, defect density, or band structure, thereby producing visually detectable color changes. By integrating responsive motifs with selective interactions or preconcentration, colorimetric sensors enable rapid, low-cost, and visually readable detection of specific gases [69].

Overall, the preceding discussion shows that technology selection for harsh-environment gas sensing should be governed by the dominant application constraint rather than by sensing performance alone. This comparison reveals a trade-off among device simplicity, analytical specificity, environmental robustness, power demand, and deployment complexity. Chemiresistive sensors occupy the low-cost, low-power, and scalable end of the design space, but their performance is more strongly constrained by environmental cross-sensitivity and signal drift. Solid-electrolyte platforms represent a high-temperature and stability-oriented route, trading robustness for higher thermal, packaging, and reference-electrode requirements. Optical methods shift the design burden from sensing-material durability to optical access, path stability, and interference correction, whereas acoustic/resonant, ionization, and mass-spectrometric methods extend mass-sensitive readout, trace analysis, and molecular identification at the expense of system compactness and deployment simplicity [70–72]. Therefore, high-temperature combustion, exhaust, and furnace-related environments generally favor solid-electrolyte sensors or remote optical platforms. In contrast, humid or corrosive atmospheres require either protected chemiresistive/solid-electrolyte interfaces or non-contact optical readout [73–75]. Low-temperature operation is more likely to benefit from optical detection, light-activated chemiresistive sensing, self-heated devices, or thermally managed sensor architectures. At the same time, vacuum and low-pressure scenarios are more compatible with optical, ionization-based, or mass-spectrometric approaches [76, 77]. For environments where temperature, pressure, humidity, and chemical composition vary simultaneously, hybrid or multimodal sensing systems that combine complementary transduction principles, reference channels, and data-fusion algorithms may offer greater reliability than a single sensing modality. However, this improvement is accompanied by increased system complexity. Thus, robust sensing in harsh environments requires matching the sensing principle to the dominant environmental stress and system-level constraint.

3. Impact of different extreme environments on gas detection

Extreme environmental conditions affect gas sensing by influencing adsorption-desorption thermodynamics, surface reaction kinetics, and transport in both gas and solid phases, thereby altering interfacial charge transfer and transduction efficiency. Variations in pressure, temperature, and humidity also influence phase stability, defect chemistry, and active-site populations, which subsequently control sensitivity, selectivity, and drift. Developing a mechanistic understanding that links these effects across relevant spatial and temporal scales is essential for the predictive design and benchmarking of sensors meant to operate in harsh environments.

Before discussing individual environmental effects, the key terms used in this chapter are defined operationally based on the conditions imposed on the sensor, gas stream, or test chamber during laboratory evaluation. Actual field environments are practical monitoring scenarios in which temperature, humidity, pressure, flow rate, and background gas composition may fluctuate simultaneously. Sensor operating temperature is the temperature of the sensing layer, heater, or transducer during measurement and should therefore be distinguished from the ambient field temperature.

3.1. Unified physicochemical framework

In previous studies, extreme environmental conditions such as high temperature, high humidity, low temperature, and vacuum are often treated as separate operating conditions, yet their effects converge on a common set of interfacial, material, device, and signal-level processes. At the sensing interface, environmental stress can affect gas diffusion, adsorption-desorption equilibrium, competitive adsorption, and surface reaction kinetics [78]. Within the sensing layer, it can alter carrier or ion transport, grain-boundary barriers, oxygen-vacancy equilibria, surface hydroxylation, catalytic activity, and defect stability [79]. At the device level, harsh environments can further accelerate electrode degradation, interfacial delamination, sealing failure, optical window contamination, and packaging aging [80]. These coupled processes ultimately manifest as response attenuation, delayed recovery, hysteresis, baseline drift, selectivity loss, and calibration mismatch. Therefore, high temperature, high humidity, low temperature, and vacuum should be viewed as different manifestations of shared physicochemical failure pathways, rather than as isolated environmental categories. The gas sensor system in harsh environments should exhibit high robustness to cope with complex environmental conditions and consistently deliver reliable detection results over an extended period [81]. Table 1 summarizes the effects of representative harsh environments on the key physicochemical and device-level factors that control gas-sensing performance.

Table 1
Dominant physicochemical trends in harsh-environment gas sensing.

Harsh environment	Adsorption/desorption	Surface reactions	Carrier/ion transport	Defect chemistry	Packaging/interface failure	Signal drift	Ref.
High temperature	lower weak-adsorbate coverage; faster desorption and recovery	faster redox kinetics; higher catalytic activity; higher side-reaction risk	higher conductivity; faster ion transport; higher leakage/noise	faster vacancy re-equilibration; higher grain-growth risk; lower morphological/phase stability	faster electrode aging; higher seal degradation; higher thermal stress	higher baseline drift; faster sensitivity decay; higher calibration mismatch	[73, 82, 83]
High humidity	higher water coverage; lower target-site availability; slower water desorption	higher hydroxylation; stronger proton-related pathways; suppressed oxygen-mediated pathways	higher protonic conduction; stronger band-bending perturbation; lower signal specificity	higher hydroxyl-defect occupancy; lower active-site accessibility; stronger hydration cycling	higher corrosion risk; higher leakage risk; lower adhesion stability	higher humidity drift; stronger hysteresis; lower selectivity	[74, 83, 84]
Low temperature	higher equilibrium adsorption; slower desorption and regeneration	slower redox kinetics; lower reaction completeness; higher activation demand	lower carrier mobility; slower ion transport; higher barrier effects	slower defect re-equilibration; higher metastable-state retention; stronger adsorbate retention	higher contraction stress; higher condensation/frost risk; lower interfacial compliance	higher baseline instability and temperature-calibration error; stronger hysteresis	[78, 85, 86]
Vacuum/low pressure	lower collision flux and adsorbate coverage; faster desorption	lower oxygen-mediated activity; stronger lattice-oxygen dependence; higher photoactivation relevance	stronger pressure-dependent resistance; altered surface depletion; weaker adsorbate-induced charge transfer	lower surface hydroxylation; altered vacancy population; stronger stoichiometry shift	higher leakage sensitivity; stronger outgassing effects; higher window-contamination risk	higher pressure-dependent baseline shift; stronger outgassing-induced drift; longer ambient-vacuum equilibration	[22, 39]

3.2. High temperature

Excessively high operating temperatures can greatly reduce gas sensor performance. Most studies define high temperature as being ≥ 300°C, which aligns with the typical 200-400°C operating range of chemiresistive MOS-based sensors. Conversely, engine/exhaust and furnace environments often reach even higher temperatures (≥600°C), since zirconia sensors typically operate around ~600-800°C, and langasite-based surface and bulk acoustic wave devices are tested near ~800-900°C [87–89]. Importantly, the relationship between sensor response and temperature is inherently nonlinear. Usually, the response increases with temperature in the low-to-mid range, where thermal activation enhances surface reactions between chemisorbed oxygen species (O_2^-, O^-, O^{2-}) and target gases. At these temperatures, higher heat accelerates charge transfer, oxygen ionization, and surface diffusion, leading to stronger modulation of the depletion or accumulation layer. However, beyond a certain temperature, sensor response sharply declines, which is mainly due to the saturation of surface reaction kinetics, and the amount of chemisorbed oxygen decreases, weakening interactions between target gases and surface-bound oxygen.

High temperatures can also cause significant microstructural changes in the sensing film, particularly in thicker films, including grain growth, pore collapse, and recrystallization. These structural changes reduce accessible surface area, block gas diffusion pathways, and ultimately decrease sensor effectiveness. Consistently, comparative studies of α-Fe_2O_3 nanostructures prepared by sol-gel and electrospinning methods have shown that temperature-dependent sensing behavior is closely associated with oxygen chemisorption sites and with analyte diffusion within the sensing-layer morphology [90]. Additionally, some sensing materials exhibit irreversible baseline conductivity drift at high temperatures, leading to the sensor's inability to fully recover its initial baseline after multiple response and recovery cycles. This irreversible behavior impacts the sensor's repeatability and long-term stability, posing a major challenge for practical applications in real-world environments [91].

Considering the materials, elevated temperature can also shift the balance among lattice oxygen, chemisorbed oxygen species and oxygen vacancies, thereby altering the density of electron donors and surface activation sites in many metal oxides [26]. This defect re-equilibration modifies surface band bending, grain-boundary barriers and heterojunction barriers, affecting both response amplitude and baseline stability. Prolonged heating further promotes grain coarsening, pore collapse, surface reconstruction and electrode-oxide interdiffusion, linking sensing-layer degradation to device-level drift and reliability loss [24].

3.3. High humidity

High-humidity conditions mainly refer to moisture-rich atmospheres above 80% relative humidity (RH) and near-saturated conditions approaching 90-100% RH, whereas ultra-low-humidity conditions below 5% RH are also considered when humidity-dependent charge transport or proton conduction is involved [74,92]. In atmospheric air at around 25°C, water concentration varies greatly with RH (6280 ppm at 20% RH and 25,740 ppm at 80% RH) [93]. Additionally, humidity levels in real-world applications are heavily influenced by environmental factors such as wind, rainfall, temperature, and diurnal and seasonal changes [94].

High humidity strongly perturbs chemiresistive baselines because water adsorption dynamically changes surface charge and resistance [95,96]. A common method to address these issues is to raise the temperature. Electrochemical gas sensors are somewhat affected by humidity. However, prolonged exposure to high-humidity conditions can decrease sensitivity, dilute the electrolyte, or cause leakage, all of which can impair the electrode reaction and sensor life [97–99]. For photoionization detectors (PIDs), high humidity can reduce ionization

efficiency and lead to condensation errors, especially when detecting volatile organic compounds (VOCs) in industrial settings. Humidity can also lower PID sensitivity, resulting in a systematic underestimation of gas concentrations at high humidity and high concentrations. To reduce interference, calibration with humidified gas or control of sample gas humidity is recommended, especially in high-concentration monitoring scenarios [100,101]. High humidity also adversely affects conductive polymer sensors, primarily through competitive adsorption of water molecules and target gases on the sensing membrane, which decreases sensitivity. Water vapor can further influence conductivity via proton transfer or by changing the distance between polymer chains, causing false alarms or unstable responses. Additionally, high humidity causes swelling of conductive polymers, increasing the space between polymer chains and reducing the efficiency of electron transfer, which can result in abnormal resistance changes or irreversible structural damage. Swelling may also alter the morphology and crystal structure of the sensing material, further impairing its ability to detect target gases. Overall, humidity not only reduces the sensitivity and selectivity of sensors but also significantly compromises their stability and repeatability [102].

Mechanistically, these effects arise from water-induced surface hydroxylation, proton-assisted conduction and humidity-dependent band-bending perturbations, which can partially screen target-gas-induced charge transfer and generate RH-dependent baseline drift [23,74]. Recent humidity-tolerant sensing studies further indicate that water can alter both interfacial transport and analyte-surface interactions, making humidity resistance a coupled surface-chemistry and charge-transport problem rather than a simple adsorption-blocking issue [103].

3.4. Low temperature

Low-temperature conditions refer to sub-zero operation, with cryogenic scenarios generally below approximately −150°C [104]. A low-temperature environment significantly hinders the performance of chemiresistive gas sensors. It mainly decreases the conductivity of the sensing material, resulting in a narrower resistance change range and reducing the sensor's ability to detect target gases. Additionally, low temperatures slow down the diffusion and adsorption of gas molecules, causing incomplete reactions, weaker sensing responses, and longer t_{res}. If the sensing mechanism relies on redox reactions or proton transfer, low temperatures will reduce reaction rates or even halt them, affecting signal accuracy. Furthermore, some sensing membrane materials may shrink, become brittle, or develop structural stress at low temperatures, weakening electrode contact stability and compromising the device's long-term reliability. Overall, these factors limit the sensitivity, response speed, and stability of resistive gas sensors in cold conditions.

At sufficiently low temperatures, thermally activated carriers in semiconducting channels can become depleted, localized or trapped at defects, grain boundaries and contacts, producing carrier-freeze-out-like transport limitations. This increases grain-boundary and contact-barrier effects, weakens adsorbate-induced charge modulation and amplifies temperature-dependent calibration errors [105,106]. In parallel, equilibrium adsorption may remain high for some gases, whereas desorption and surface regeneration become slower, leading to stronger hysteresis and incomplete recovery [107].

3.5. Vacuum

Vacuum and low-pressure conditions are defined by absolute pressure, ranging from reduced pressure below atmospheric pressure to medium vacuum of 100-0.1 Pa, high vacuum of 0.1-10^{-5} Pa, and ultra-high vacuum below 10^{-5} Pa [108]. These pressure regimes reduce molecular density, gas-surface collisions, and oxygen partial pressure, thereby altering adsorption- and redox-based sensing processes.

Gas sensing in a vacuum environment presents several challenges. Vacuum weakens adsorption-based signals by lowering gas density and gas-surface collision flux [109,110]. The reduced effective collision of gas molecules results in longer t_{res} and increased calibration and repeatability errors [111–113]. Some sensing materials may also deteriorate due to changes in surface structure. Therefore, the above factors need to be considered in the design of gas sensors suitable for vacuum conditions. Otherwise, alternative detection techniques, such as mass spectrometry and spectroscopy, should be employed.

For metal-oxide sensors, reduced oxygen partial pressure suppresses the formation of surface reactive oxygen species and shifts the equilibrium among adsorbed oxygen, lattice oxygen and oxygen vacancies [26,84]. Consequently, conventional oxygen-mediated chemiresistive pathways become less effective, while the signal becomes more sensitive to pressure-dependent surface stoichiometry, leakage, outgassing and background desorption [22]. Oxygen-independent reaction pathways, lattice-oxygen participation or photoactivation can partly compensate for this limitation, but pressure-resolved calibration remains necessary for quantitative reliability [114].

4. Applications of gas sensing technologies under extreme conditions

This section examines the use of gas-sensing technologies under four extreme conditions: high temperature, high humidity, low temperature, and vacuum. Each subsection reviews sensing performance, challenges, practical operating conditions and typical applications. A comparison summary is also included in Table 2 to emphasize key findings and reported sensor adaptations.

4.1. High-temperature gas sensing

High-temperature toxic-gas monitoring requires sensors that retain calibration and contact integrity at 350-600°C [131]. Such environments also pose significant challenges to the stability and lifespan of gas sensors. Traditional sensor packages made of metal-glass composites, like Kovar alloys with electroless nickel immersion gold (ENIG) coatings, are susceptible to oxidation, corrosion, and phosphorus-induced recrystallization at elevated temperatures (≥250°C), which can cause electrical contact degradation and functional failure. Additionally, silicon-based membrane microheaters break down under thermal stress above 700°C, resulting in structural damage and sensor failure. These issues include delamination, cracked metallization, and compromised hermeticity, which restrict the operating range of conventional sensors to below 150°C. Experimental evaluations have confirmed that standard sensors exhibit total plating oxidation and package deformation after exposure to 850°C for just 10 min, rendering them unsuitable for harsh air environments [132]. These findings highlight the urgent need for high-temperature-tolerant materials and packaging technologies to enable reliable sensing in extreme thermal applications.

To address extreme environments like high temperatures, Wang et al. developed a self-powered NH_3 sensor by integrating $Ti_3C_2T_x/MoS_2$ nanoheterostructures into electrospun cellulose nanofiber membranes and coupling them with a triboelectric nanogenerator (TENG). The device maintained >90% $PM_{0.3}$ filtration efficiency and a stable electrical output at 100°C and 99% RH, while detecting NH_3 with a LoD of 0.1 ppm and a response time of 2 s to 100 ppm NH_3 [115]. This study indicates that long-term sensing in thermally coupled environments benefits from multifunctional device integration, where the sensing membrane, filtration layer, and energy-harvesting unit are designed as a single operational stack.

In parallel, oxide composition and morphology engineering provides a material-level route to stabilize high-temperature chemiresistive sensing. Qin et al. demonstrated a MOF-derived 3 mol% Mn-doped In_2O_3 hollow nanotube sensor for H_2 detection. The high surface area of 122 m^2/g and oxygen-vacancy-rich structure enabled operation at 360°C, with an LoD of 25 ppb, a detection range of 25 ppb-500 ppm, a t_{res}/t_{rec} of 4/15 s, and stable operation over 30 days [116]. The work

Table 2
Applications of gas sensing technologies under extreme conditions.

Extreme environment	Sensor type	Materials	Synthesis method	Target gas	Operation condition	Detection concentration	Sensing performance	t_{res}/t_{rec}	Ref.
Primarily high temperature	Triboelectric nanogenerator	Cellulose diacetate, $Ti_3C_2T_x$ MXene, MoS_2	Hydrothermal, electrospinning, thermal treatment	NH_3	≤ 100°C, 99% RH	0.1-100 ppm	[b]86% at 100 ppm	2 s/3 s (100 ppm); 11.2 s/4 s (0.1 ppm)	[115]
	Chemiresistive gas sensor	3 mol% Mn-doped In_2O_3 hollow nanotubes	Solvothermal, annealing	H_2	280°C-400°C, optimal at 360°C	0.0025-500 ppm	[a]1.93 at 20 ppm, [a]2.57 at 50 ppm (360°C)	4 s/15 s (20 ppm)	[116]
	Mixed-potential ceramic solid electrolyte sensor	YSZ-based solid electrolyte, $ZnFe_2O_4/ZnCr_2O_4$	Tape-casting, screen-printing, sintering	NO_x	13-14% O_2, 3% moisture, >800°C exhaust	300-1500 ppm	Stable signal variation with NO_x concentration; minimal drift or noise	1.2 s/- (1350-1500 ppm) 2.29 s/- (300 ppm)	[117]
	ATR-FTIR (mid-infrared sensor)	Kraton G-1650, Polyisobutylene (PIB)	Drop-casting from $CHCl_3$	Toluene, Naphthalene	22-80°C; pressure up to 137.9 bar	8-35 ppm (Toluene); ≤ 14.4 ppm (Naphthalene)	Kraton G-1650 was 1.85 times more sensitive than PIB at 60°C	~20-25 min/- for Toluene; ~50-60 min/- for Naphthalene at 40°C	[118]
	Chemiresistive gas sensor	Pt-decorated SnO_2	Ink Dispensing, annealing	CH_4	100 ppm H_2S treatment for 10 min at 400°C	100 ppm	[a]Increased from 1.23 to 1.51	9.6 s/17.4 s	[119]
				NH_3			[a]Increased from 1.10 to 2.4	2.6 s/3.7 s	
				HCHO			[a]Increased from 1.03 to 2.5	3.3 s/3.5 s	
	Chemiresistive gas sensor	Pd-Pt/SiC on porous silicon	RF magnetron sputtering	H_2	Dry air, elevated temp (up to 500°C)	5-500 ppm	[d]71% at 100 ppm H_2	21 s/35 s (100 ppm)	[120]
High humidity	Chemiresistive gas sensors	C/WO_3/Bi_2WO_6	Hydrothermal	Benzaldehyde	40% RH~90% RH	100 ppm	5.49% response drift	−/−	[121]
	Graphene Field Effect Transistor	Peptides (GR3R, P1, LBP3), Graphene	Peptide self-assembly on graphene	D-limonene, L-limonene, (−)-menthol, methyl salicylate, ethyl propionate	19% RH-54% RH	LoD≈3.0 ppm D-limonene: (untreated), ~7.5 ppm (LBP3)	The response of D-limonene is 35-fold higher over L-limonene	~10 min/ 10 min	[122]
	Chemiresistive gas sensor	$FASnI_3/(BA)_2SnI_4/SnO_2$	Solution synthesis and calcination	HCHO	78% RH	50 ppm	[a]32.5	67 s/81 s	[123]
	Chemiresistive gas sensor	Tellurene (2D Te nanoflakes)	Hydrothermal	NO_2	0% RH-80% RH	10 ppm	[d]~45% stably at 80% RH	14 s/79 s (80% RH)	[124]
	Colorimetric gas sensor	CH_3-Cu-BTC (methyl-functionalized Cu-BTC MOF)	Solvothermal	NH_3	75% RH	≥5 ppm	Visible color change from ruby green to blue	Color switch completed in 4 min	[125]
	Chemiresistive gas sensor	$ReS_2/Ti_3C_2T_x$	One-pot hydrothermal	NH_3	15% RH-85% RH	1-500 ppm	[d]12.7% at 85% RH (10 ppm)	~30 s/~45 s (15% RH)	[103]
Low temperature (partial co-existence of high humidity)	NDIR	MEMS IR emitter, MEMS thermopile detector, gold-coated curved mirror, waterproof breathable film	Assembled MEMS components with reflective gas chamber	CO_2	−20°C to 60°C; 0-100% RH	0.5%-20%	Optical coupling efficiency (~48%), long-term drift (134 ppm/month), good accuracy (±50 ppm)	22 s/38 s	[126]
	Optical hydrogen sensors	$Ta_{88}Ru_{12}$	Magnetron sputtering	H_2	−60°C	3%	The largest optical contrast	6 s/-	[105]
	Organohydrogel-based 2-electrode sensor	Polyvinyl alcohol-cellulose nanofibril double-network organohydrogel	One-pot polymerization	NO_2	RT and below (down to −20°C)	0.004-10 ppm, LoD = 2.23 ppb	[c]372%/ppm at RT under strain; [c]112%/ppm at −20°C	41/144 s (250 ppb)	[127]
	Chemiresistive gas sensors	Polypyrrole-loaded $Sn_{1-x}Sb_xO_2$ nanocubes	Co-precipitation method, magnetic stirring	NH_3	−21°C −78°C	20 ppm	[a]4 [a]4	11 s/71 s 15 s/80 s	[128]

(*continued on next page*)

Table 2 (*continued*)

Extreme environment	Sensor type	Materials	Synthesis method	Target gas	Operation condition	Detection concentration	Sensing performance	t_{res}/t_{rec}	Ref.
	Chemiresistive gas sensors	Sb-Doped SnO_2@g-C_3N_4	Hydrothermal	H_2S	−20 °C	2 ppm	[a]20.1	14 s/-	[106]
	Photoactivated chemiresistive gas sensor	N-doped carbon dots/SnS_2	Solvothermal, hydrothermal	NO_2	Oxygen-free and low temperature (238 K)	0.01 ppb-10 ppm	[d]3.1% at 0.1 ppm	11 s/139 s (1 ppm)	[107]
Vacuum	Amperometric/ Potentiometric	YSZ (8 mol%) tube, Pt electrodes	DC sputtering	Hydrocarbons (e.g., toluene, butane)	Ultra-high vacuum (~3×10^{-9} mbar)	Sub-ppm to ppm level	Sensitive to trace hydrocarbons	−/−	[129]
	Ultraviolet-assisted chemiresistive sensor	SnO_2-CuO, ZnO-CuO	Sol-gel	H_2S	3×10^{-3} Pa	0.1-25 ppm	[a]293@3 ppm for SnO_2-CuO	7.3 s/- (under ultraviolet)	[22]
	SERS sensor	Ag/Si 3D substrate; Ag/ silicon membrane; Micropump	Electroless silver deposition	Hydrazine	Spacecraft interior; N_2-purged gas chamber	0.1 ppm	Characteristic SERS peaks were detected	−/−	[130]
	Chemiresistive MEMS sensor	Core-shell SnO_2@Ag_2O composite	Co-precipitation, drop coating, vacuum drying	H_2S	1×10^{-5} Pa, −20°C	1 ppm	[a]7.6	15.3 s/-	[114]

TEOS: tetraethyl orthosilicate; MEMS: micro-electromechanical systems; MOF: metal-organic framework; ATR-FTIR: attenuated total reflection Fourier-transform infrared spectroscopy; RF: radio-frequency; RT: room temperature.

[a] $S=R_g/R_a$ or $S=R_a/R_g$, R_a is the initial resistance in the air, and R_g is the resistance in the target gas.

[b] $S = |V\text{-}V_0|/V_0 \times 100\%$, where V_0 and V are the initial voltage without contacting the target gas and the voltage contacting the target gas, respectively.

[c] $S = |I\text{-}I_0|/I_0 \times 100\%$, where I_0 and I are the initial current without contacting the target gas and the current contacting the target gas, respectively.

[d] $S = |R_g\text{-}R_a|/R_a \times 100\%$, where R_a is the initial resistance in the air and R_g is the resistance in the target gas.

highlights the effectiveness of structural and electronic modulation strategies, especially MOF-derived architectures and transition metal doping, in overcoming the limits of traditional metal oxide sensors. This paves the way for advanced gas sensing in high-temperature and chemically aggressive environments.

Ha et al. presented the development and performance evaluation of a high-temperature-stable NO_x sensor specifically designed for automotive exhaust gas monitoring. This research addresses critical challenges associated with gas sensing in harsh environments, particularly those involving temperatures exceeding 800°C, corrosive exhaust gas compositions, and the need for real-time, selective detection of NO and NO_2. The proposed sensor uses a ceramic solid-state electrolyte (YSZ) and a mixed-potential sensing mechanism to overcome the limitations of conventional amperometric and resistive sensors, which are prone to signal instability and material degradation at high temperatures. Novel sensing electrodes based on $ZnFe_2O_4$ and $ZnCr_2O_4$ were synthesized and screen-printed onto multilayer ceramic green sheets, including internal heaters, porous diffusion barriers, and protective insulation. Extensive structural, thermal, and electrochemical analyses confirmed the sensor's integrity and performance. Notably, the integrated heater maintained operating temperatures above 800°C, and the sensor showed fast response times (1.2 s to 2.29 s) across NO_x concentrations ranging from 300 ppm to 1500 ppm. These results outperformed many traditional solid electrolyte sensors and approached the performance of commercial leaders like NGK [117]. This study demonstrates a robust approach for designing gas sensors that can operate reliably in high-temperature automotive environments over long periods. It emphasizes the importance of material choice, layered ceramic engineering, and optimized sensor architecture for dependable gas detection under extreme conditions.

Heath et al. focused on developing durable MIR attenuated total reflectance (MIR-ATR) spectroscopic sensors for detecting trace hydrocarbons in aquatic environments under high-temperature and high-pressure conditions, such as in oil spill monitoring or downhole groundwater surveillance. The authors explore styrenic ABA block copolymers, especially Kraton G-1650, as advanced sensing membrane materials. These polymers exhibit microphase separation, combining rubbery, low-Tg midblocks that facilitate hydrocarbon diffusion with glassy, high-Tg styrenic endblocks that provide thermal and mechanical stability, making them suitable for harsh environments. Experimental results show that Kraton G-1650 exhibits significantly higher sensitivity and a faster response than conventional PIB, with stable and linear performance maintained up to 60°C under 137.9 bar, although delamination occurred at higher temperature because of interfacial adhesion and thermal-expansion mismatch [118]. This work highlights the potential of styrenic block copolymers for enabling reliable gas sensing in extreme environments. It also underscores key challenges, such as improving film-substrate adhesion and reducing thermally induced stress, which are necessary to expand sensor applications in high-temperature settings like deep-sea monitoring, unconventional gas extraction, and geothermal systems.

In addition, Chen et al. reported a novel strategy to enhance the performance of metal oxide gas sensors under high-temperature, sulfur-rich conditions by H_2S treatment. Contrary to the conventional poisoning effect, brief exposure to H_2S at 400°C significantly improved the sensing response of SnO_2-based sensors to multiple reducing gases (e.g., CO, NH_3, CH_4, HCHO), with response enhancements up to 270%. This effect is attributed to the formation of surface metal sulfide and sulfate species, which facilitate electronic sensitization and modulate charge transfer during gas detection [119]. The enhancement is temperature-dependent and gradually attenuates over time, offering valuable insights into the design of high-temperature gas sensors for harsh environments through controlled surface modification.

Overall, current high-temperature gas-sensing studies improve robustness primarily through thermally stable sensing layers and ceramic solid-electrolyte architectures. These strategies help preserve

gas-accessible structures, charge-transfer pathways and high-temperature response stability, but they do not fully resolve long-term drift, electrode degradation and package-level failure. Future work should evaluate sensing layers alongside high-temperature contacts, thermally matched packaging and repeated thermal-cycling tests that track drift, adhesion and electrode continuity.

4.2. High-humidity gas sensing

As MOS-based gas sensors suffer significant signal drift in humid environments [74,133], the mechanisms underlying this drift require clarification. The widely accepted sensing mechanism of MOS-based gas sensors primarily involves the adsorption of oxygen species (O_2^-, O^-, and O^{2-}) on the semiconductor surface [134,135]. Under humid conditions, H_2O molecules undergo competitive chemisorption at the same active sites as oxygen species on the material surface. This process results in the release of electrons previously captured by adsorbed oxygen back into the metal oxide lattice (Fig. 6a-b), as illustrated by the following reaction (1) [136]:

$$H_2O + 2M_m + O_{ad}^- \leftrightarrow 2\left(M_m^+ - OH\right) + e^- + S \quad (1)$$

where M denotes a metal elements in MOS, M_m refers the site of M on the surface, O_{ad}^- is related to ion-adsorbed oxygen species, e^- refers to the electron, $\left(M_m^+ - OH\right)$ is a terminal hydroxyl group while S is a surface site for chemically adsorbing oxygen. Under increasing humidity conditions during gas detection, the interaction between H_2O molecules and the sensing layer undergoes a progressive transition from isolated chemisorption to a combined chemisorption-physisorption mechanism (Fig. 6c) [137]. This transition facilitates proton-hopping conduction, significantly reduces the electrical resistance, and compromises sensing accuracy [138]. Consequently, competitive adsorption effects emerge,

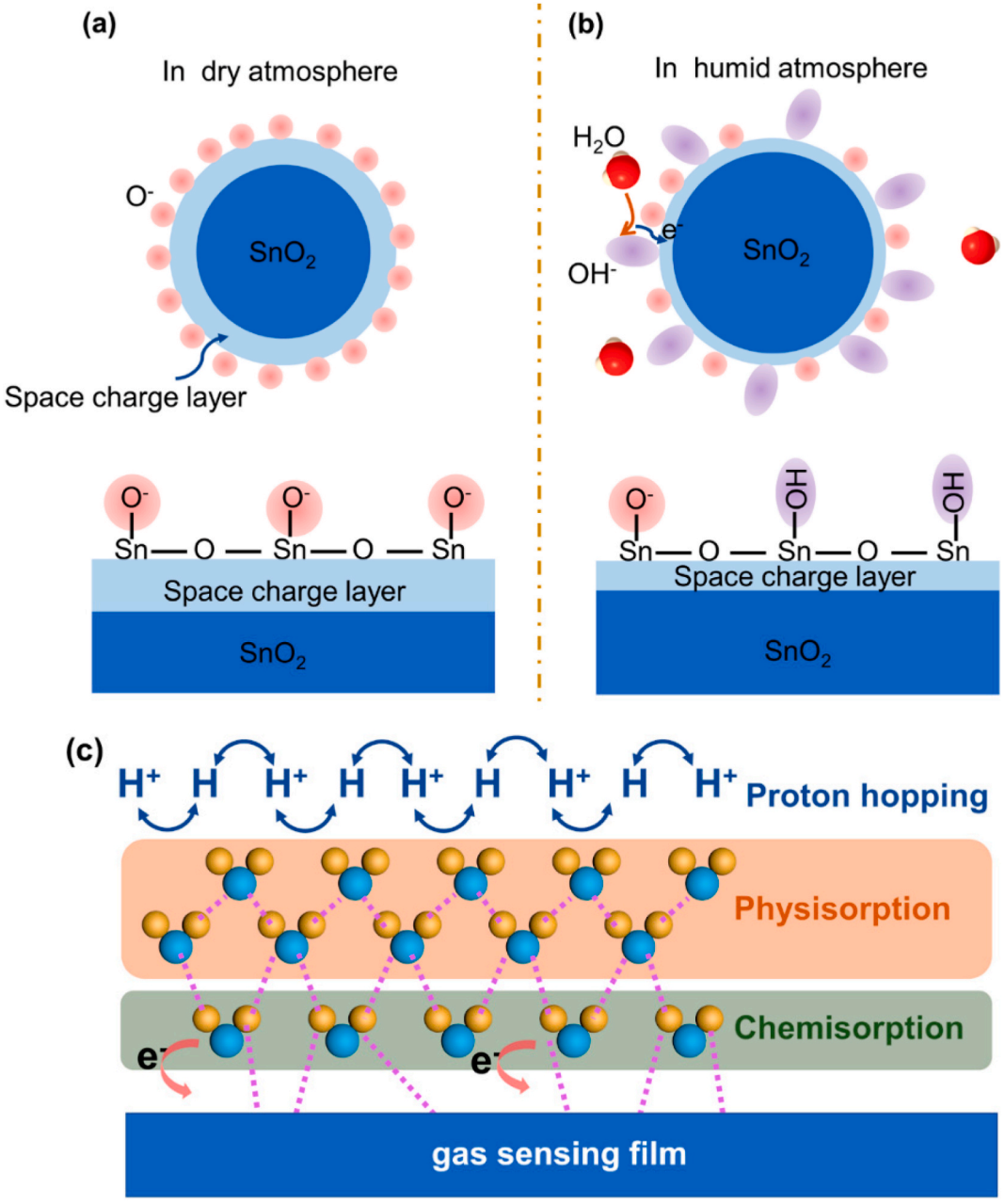

Fig. 6. Schematic diagram of the gas-sensing model for SnO_2 in (a) dry atmosphere and (b) humid atmosphere. (c) Schematic illustration of chemisorption and physisorption of water molecules in high-humidity conditions. Reproduced from Ref. [74], MDPI, open access under CC BY license.

ultimately degrading the sensor's sensitivity [74,139].

Yamazaki et al. demonstrated selective and stable detection of biogenic VOCs (BVOCs) in high-humidity environments using peptide-functionalized graphene field-effect transistors (GFETs). Traditional graphene-based gas sensors are highly sensitive but often suffer from water vapor-induced instability, which limits their reliability in humid conditions. The peptide monolayers function simultaneously as odorant-recognition layers and humidity buffers, enabling stable operation at RH levels up to 54% and suppressing water-induced fluctuations in conductivity. Notably, the LBP3-modified GFET showed humidity-assisted enantioselective detection of limonene, with a 35-fold higher response to D-limonene than to L-limonene, far above the less-than-twofold selectivity typically reported for previous graphene sensors. The sensors also distinguished various BVOCs, including menthol, methyl salicylate, and ethyl propionate, with responses that depended on peptide type and humidity level. Multivariate analyses, including principal component analysis (PCA) and hierarchical cluster analysis (HCA), confirmed the sensors' ability to classify odorants accurately under moist conditions [122].

In response to the challenge of gas sensing in high-humidity conditions, Wang et al. also introduced a novel strategy to improve sensor stability and performance using 2D/3D organic-inorganic hybrid perovskite materials. Conventional 3D perovskites like $FASnI_3$ are highly sensitive to formaldehyde but deteriorate severely when RH exceeds 50%. To solve this, the researchers added a hydrophobic 2D perovskite, $(C_4H_9NH_3)_2SnI_4$, into the $FASnI_3$ matrix, and partially oxidized the composite to form FA+10BA-S, a heterostructure with SnO_2. The hydrophobic 2D part effectively mitigated moisture interference by repelling water molecules, helping to preserve the sensor's integrity and performance. At 78% RH, the sensor maintained 63% of its response with minimal degradation after 24 h, showing excellent moisture resistance. Additionally, forming oxygen vacancies and heterojunctions enhanced gas adsorption and charge transfer, leading to a high response of 50.6 to 50 ppm HCHO, a short t_{res}/t_{rec} (67/81 s), and a low LoD (220 ppb) at 50°C [123]. This work highlights the potential of structural engineering with hydrophobic perovskite phases as a sturdy solution for gas sensing in humid and harsh conditions.

Je et al. reported a tellurene-based chemiresistive NO_2 gas sensor that works effectively at room temperature under high humidity, addressing a key challenge in real-world applications. While many gas sensors perform poorly in humid environments, this tellurium sensor shows both high sensitivity and detection unaffected by humidity. Made using a hydrothermal method, it features a flake-like 2D structure with high crystallinity and excellent intrinsic conductivity. It responded to NO_2 very quickly, with a t_{res} of 14 s and a LoD as low as 19 ppb, even at RH up to 80%. Interestingly, humidity actually improves performance by enhancing charge transfer, forming additional conduction pathways and reducing t_{rec}. This stability against humidity fluctuations comes from the air-stable semimetallic nature of tellurene and its unique surface interactions with NO_2 [124]. These findings suggest tellurene is a promising material for reliable, high-speed, low-power gas sensors suitable for harsh and variable environments, such as wearable breath analyzers or ambient air monitors.

Wang et al. proposed a new approach to tackle the challenges of gas sensing in high-humidity environments by developing a methyl-functionalized copper-based metal-organic framework (CH_3-Cu-BTC) for colorimetric detection of NH_3. Exhaled NH_3, a biomarker for kidney and liver diseases, is hard to detect accurately because of water vapor at high RH. By adding hydrophobic methyl groups into the MOF, the CH_3-Cu-BTC shows better selectivity and sensitivity to NH_3, even at 75% RH, with a visible color change from ruby green to blue, detectable at concentrations as low as 5 ppm. Density functional theory (DFT) calculations show that NH_3 interacts more strongly with the Cu^{2+} centers than H_2O does, changing their coordination environment and triggering the color change. The material is also highly stable and reusable, maintaining performance over multiple cycles. Furthermore, CH_3-Cu-BTC can distinguish between exhaled air from healthy individuals and patients, showing its potential for non-invasive, real-time diagnosis in humid physiological conditions [125]. This work offers a promising strategy for designing gas sensors that work well in moisture-rich environments.

Collectively, current high-humidity strategies reduce water interference through humidity-buffering interfaces, hydrophobic structures, moisture-tolerant conductive channels, and target-specific binding sites. These approaches improve selectivity and baseline stability in humid atmospheres. However, RH-dependent response variation remains difficult to eliminate because water still participates in adsorption, surface charge transfer, and transport processes. Future work should combine gas-permeable anti-humidity barriers with integrated humidity/temperature reference channels and RH-dependent calibration.

4.3. Low-temperature gas sensing

In gas sensing, low temperature generally refers to the sensor's operating environment at relatively low temperatures. Specifically, low temperature usually means below room temperature (25°C). Low temperatures are crucial for maintaining the quality and extending the shelf life of perishable food products. For gas sensing in food preservation cabinets, biological cabinets, and other areas, a low-temperature detection condition is necessary [140,141]. Therefore, Xu et al. proposed a compact NDIR gas sensor with a microelectromechanical systems (MEMS) emitter and a gas cell with high optical coupling efficiency (~48%) to detect CO_2 at low temperatures (down to −20°C). They reduced the sensor's size to 24 mm × 8 mm × 8 mm (length × width × height), which is only 30% of a standard NDIR sensor with the same detection resolution. This reduction improves temperature regulation efficiency. The detection results show that the sensor's CO_2 accuracy remains the same at −20°C and 20°C, with a t_{res} of only 22 s, highlighting the importance of sensor design for low-temperature gas detection [126]. Yuan et al. studied the reliable performance of optical hydrogen sensors based on metal hydrides, capable of efficient hydrogen detection at temperatures as low as −60°C, as shown in Fig. 7. In situ X-ray diffraction (XRD) analysis confirmed no phase transitions, plastic deformation, or hysteresis during hydrogen exposure, ensuring stable and reversible optical responses. Although optical contrast decreases with temperature, the $Ta_{88}Ru_{12}$ sensor performs well, maintaining high optical contrast and a quick t_{res} of 6 s at −60°C. Kinetic analysis points to surface-limited processes like hydrogen dissociation as the main rate-determining steps. These results support the use of metal hydride-based optical sensors in low-temperature environments and highlight their potential in extreme conditions [105].

Ding et al. reported a high-performance NO_2 gas sensor designed for operation in harsh environments, especially at sub-zero temperatures. The sensor uses a self-healable, recyclable, and ultra-stretchable polyvinyl alcohol-cellulose nanofibril (PVA-CNF) double-network organohydrogel, which incorporates glycerol as an antifreeze agent to maintain flexibility and functionality down to −78.2°C. It exhibits exceptional sensitivity (372%/ppm) and a low LoD (2.23 ppb), along with excellent selectivity and stability even under high humidity and mechanical deformation such as stretching, bending, and twisting. The organohydrogel structure also ensures outstanding mechanical durability, including self-healing, remoldability, and high fracture energy. These features enable the sensor to recover its gas-sensing performance after mechanical damage and sustain long-term operation. The sensing mechanism relies on redox reactions at the gas-gel-electrode interface, which are enhanced by humidity and tensile strain. Additionally, the sensor is integrated with a low-power wireless circuit capable of real-time NO_2 detection and alarm functions, demonstrating its practical potential for wearable, flexible, and autonomous monitoring systems [127]. This work effectively overcomes the main limitations of traditional chemiresistive gas sensors in cold or variable environments, offering a viable path toward developing robust gas-sensing technologies

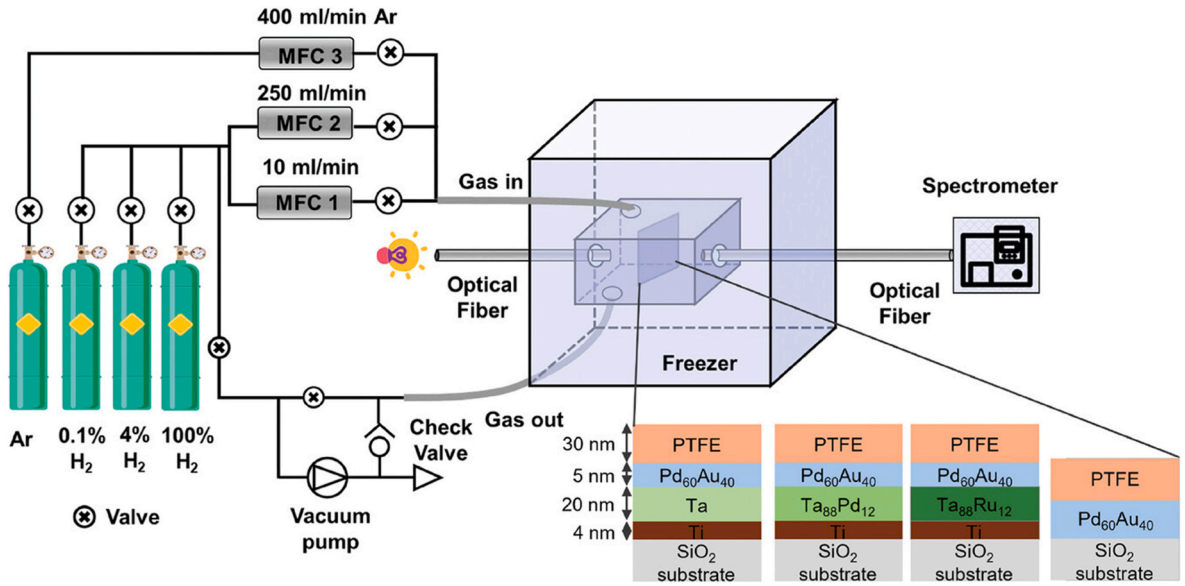

Fig. 7. Schematic diagram of the experimental configuration designed for quantifying the change in transmittance of metal hydride thin films when subjected to varying hydrogen concentrations at low temperatures. The inset shows a schematic representation of the samples. Reproduced from Ref. [105], John Wiley and Sons, open access under CC BY license.

for extreme conditions.

Chakraborty and Mondal reported a hybrid chemiresistive NH_3 sensor capable of sub-zero operation. The sensing material was prepared by *in situ* polymerization of polypyrrole (PPY) on antimony-doped tin oxide ($Sn_{1-x}Sb_xO_2$, specifically ATO_0.05), forming a conductive microporous network that supports gas adsorption and carrier transport at low temperature. The composite sensor achieved stable, selective NH_3 detection at −78°C, with a detection range of 1-20 ppm and a resistance change of up to fourfold. Unlike conventional oxygen-mediated chemiresistive sensing, the response was attributed to an exciton-like electron-hole-pair formation and recombination process, enabling operation under oxygen-limited conditions. The sensor also showed 18-month stability and good selectivity toward NH_3 over CO, ethanol, and acetone [128]. This work is the first reported example of chemiresistive gas sensing at sub-zero temperatures, opening the door to low-cost, miniaturized gas sensors suitable for harsh environments such as cold-chain logistics, biomedical storage, and polar-region monitoring.

Addressing the ongoing challenges of gas sensing at subzero temperatures, Pi et al. introduced a novel strategy that significantly improves the performance of semiconductor gas sensors in harsh environments. Conventional MOS sensors, such as SnO_2, suffer from limited charge-carrier mobility and insufficient chemisorbed oxygen at low temperatures, resulting in poor sensitivity. To solve this problem, the authors engineered a UV-assisted chemiresistive sensor by integrating Sb-doped SnO_2 microspheres with net-like g-C_3N_4, forming a type-II heterojunction that enhances the separation and transport of photogenerated charge carriers. Under UV illumination, the sensor benefits from increased surface carrier density and activation of oxygen species, enabling efficient 2 ppm H_2S detection at −20°C with a fast t_{res} of 14 s and a high response value of 20.1. The sensor also demonstrates strong selectivity, long-term stability over 20 days, and consistent performance. These experimental results are further validated by DFT calculations, which confirm improved adsorption energies and charge activity under UV excitation [106]. This work provides a promising, energy-efficient route to enabling semiconductor gas-sensing technologies to operate effectively at extremely low temperatures, with broad implications for deep-space missions and other demanding environments.

Taken together, current low-temperature strategies maintain sensing output primarily through optical readout, anti-freezing conductive matrices, and photoactivated semiconductor interfaces. These approaches extend sensing into sub-zero conditions and reduce the need for global heating, but incomplete recovery, condensation-related errors, and calibration drift remain major limitations. Future work should pair localized activation with anti-condensation inlet design and repeated freeze-thaw validation to verify stability under cyclic cold exposure.

4.4. *Vacuum gas sensing*

This section examines recent research on gas detection in vacuum environments in detail. First, the structure and performance of the CuO-based heterojunction gas sensor are illustrated under high vacuum conditions (3×10^{-3} Pa), as shown in Fig. 8. By constructing SnO_2-CuO and ZnO-CuO p-n heterojunctions that operate under 365 nm UV-LED illumination, the sensor can efficiently detect H_2S gas even in oxygen-free environments. Specifically, the reaction of CuO with H_2S produces conductive CuS (Fig. 8a), which is facilitated by UV light promoting the generation of electron-hole pairs and enhancing the gas reaction activity (Fig. 8b), leading to significant changes in the sensor's resistance. The sensor shows excellent selectivity for H_2S among various gases (Fig. 8c) and maintains good stability over a 7-day testing period (Fig. 8d). Comparing conditions with and without UV-LED illumination demonstrates that UV excitation greatly enhances response value and response speed (Fig. 8e). The response increases non-linearly with higher concentrations (Fig. 8f), and the LoD reaches 100 ppb (Fig. 8g). Additionally, different CuO doping levels substantially affect response performance, with 9% providing optimal results (Fig. 8h). Overall, these findings suggest that this sensor design has excellent H_2S detection capabilities under vacuum and at room temperature, making it suitable for extreme environments such as space exploration [22].

Kyriakou et al. studied hydrocarbon contamination under ultra-high vacuum (UHV), particularly in extreme ultraviolet (EUV) lithography systems, where carbon deposition degrades Ru-capped multilayer mirrors. They showed that photoelectrons, rather than EUV photons, primarily drive carbon buildup, with toluene and long-chain alkanes producing higher contamination rates due to longer surface residence times. To monitor trace hydrocarbons at low pressure, the authors developed a YSZ-based solid-electrolyte sensor with a Pt working electrode exposed to UHV and a reference electrode maintained at

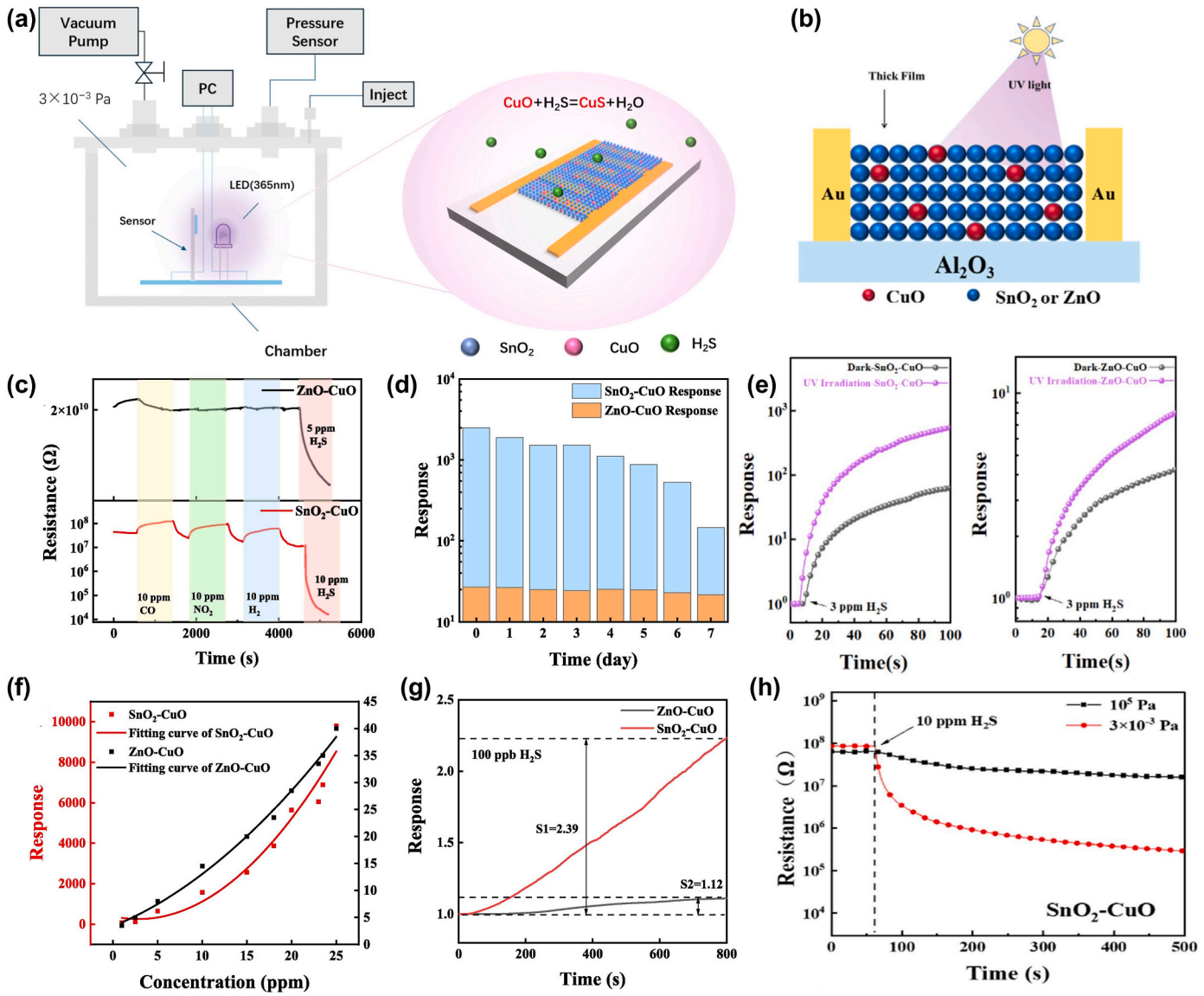

Fig. 8. (a) Schematic diagram of the gas sensor setup for H_2S detection in vacuum under UV-LED irradiation. (b) Schematic of the gas sensor setup. (c) Selectivity of SnO_2-CuO and ZnO-CuO sensors for 10 ppm of various gases (CO, NO_2, H_2, H_2S) and (d) stability of sensor responses over 7 days, with each cycle involving 24 h of recovery in atmospheric conditions under UV-LED in 3×10^{-3} Pa. (e) ZnO-CuO and SnO_2-CuO response to 3 ppm H_2S under vacuum (3×10^{-3} Pa) with and without UV-LED. (f) Sensitivity as a function of H_2S concentration (0-25 ppm) and (g) LoDs for H_2S, showing resistance changes over time for sensors under UV-LED in 3×10^{-3} Pa. (h) ZnO-CuO response to 7.5 ppm H_2S with varying CuO concentrations (0.1%-0.9%) with UV-LED under high vacuum conditions. Reproduced with permission from Ref. [22], Copyright© 2025, Elsevier.

atmospheric pressure. Operated at ~873 K, the sensor worked in both potentiometric and amperometric modes. Open-circuit potential shifts reflected hydrocarbon adsorption, whereas electrochemical oxygen-pumping current quantified hydrocarbon concentration. The sensor detected hydrocarbons at pressures as low as 10^{-9} mbar, and bimetallic Pt-Au electrodes improved selectivity among alkanes, alkenes, and aromatics through tailored surface compositions [129]. These results show the potential for deploying compact, high-sensitivity gas sensors in harsh vacuum environments for contamination monitoring and real-time process control in advanced manufacturing systems.

Regarding space missions, detecting VOCs and trace contaminants under vacuum or low-pressure conditions poses significant challenges due to minimal molecular adsorption and strict sensitivity needs. Snitka et al. introduced a SERS sensor platform designed for ultra-sensitive molecular detection in harsh environments. The sensor uses Ag nanoparticle-coated porous silicon membranes, fabricated through electrochemical etching and electroless Ag deposition, to generate dense plasmonic "hot spots" that boost signals without needing strong molecular adsorption. To address the low density of gas molecules in vacuum, a micropump is integrated to actively pull analytes through the SERS-active membrane, increasing the chance of interaction and detection sensitivity. The system successfully detected hydrazine vapor at 0.1 ppm and non-polar anisole vapor at 0.5 ppb, confirming its high performance under simulated low-pressure conditions. Its compatibility with portable Raman spectrometers enables real-time, on-site monitoring without complicated sample preparation or sample return, making it ideal for spacecraft cabin air monitoring, planetary exploration, and autonomous environmental diagnostics in space [130]. These findings highlight the potential of SERS-based platforms as next-generation gas sensing solutions for extreme aerospace environments.

Pi et al. presented a MEMS-based chemiresistive H_2S gas sensor using a core-shell SnO_2@Ag_2O composite for operation under vacuum and low temperature. The sensor operated at pressures as low as 1×10^{-5} Pa and

at −20°C, mimicking space environments. Traditional MOS gas sensors often fail under such conditions because they rely on surface-adsorbed oxygen species that desorb in vacuum. In this design, SnO_2 microspheres provide H_2S adsorption sites, while the Ag_2O shell reacts directly with adsorbed H_2S to form conductive Ag_2S. This adsorption-reaction coupled mechanism enables a resistance response without relying on ambient oxygen. The SnO_2@Ag_2O sensor showed a response time of 15.3 s, high selectivity, and a detection range of 100 ppb-10 ppm for H_2S, with minimal cross-sensitivity to NH_3 and H_2O (both common in lunar soil). The study also used electron paramagnetic resonance (EPR) spectroscopy to examine pressure-dependent oxygen desorption, confirming the loss of chemisorbed oxygen with increasing vacuum [114]. This work demonstrates that gas detection is possible in oxygen-free environments and offers a promising approach for next-generation space-compatible gas sensors.

Overall, current vacuum gas-sensing strategies compensate for low molecular flux and oxygen depletion through oxygen-independent reactions, photoactivation, plasmonic readout, and active analyte delivery. These approaches enable low-pressure detection, but calibration mismatches, leakage effects, and long equilibration times still limit quantitative reliability. Future work should combine oxygen-independent sensing chemistry with active sampling, pressure-resolved calibration, and low-outgassing device packaging.

5. Design considerations toward continuous harsh environment detection

Future advances in harsh-environment gas sensing will be driven by application-specific performance standards and architectures that turn laboratory breakthroughs into reliable field devices. This section covers stability challenges in gas detection. It compiles solution strategies and design guidance for upcoming sensors operating in extreme conditions (Fig. 9). Accurate measurement must be maintained under combined stresses such as heat, pressure, moisture, corrosive media, and vibration, while ensuring short t_{res}, low power consumption, and demonstrated selectivity in real-world environments. The most promising approach involves integrated design that combines durable transducers like solid electrolytes, wide bandgap electronics, and high-temperature acoustic devices with catalytic or permselective interfaces, conditioned sampling, and multilayer barrier systems, alongside lightweight edge analytics that maintain calibration across operational conditions. Evaluation should focus on deployment metrics, including LoDs amid complex backgrounds, dynamic accuracy during load changes, system uptime, service intervals, and compliance with safety standards. These trends point toward modular, networked platforms for hydrogen handling, ammonia/electrofuels, high-temperature process control, geothermal monitoring and aerospace propulsion.

Current evidence from applications further illustrates this laboratory-to-field gap. Zirconia-based electrochemical sensors are mature platforms for oxygen monitoring, combustion control, and exhaust after-treatment systems, and optical systems have enabled *in situ* monitoring in hydrothermal environments [54,142,143]. However, frontier scenarios, such as Venus-surface exploration, remain difficult to access directly, and high-fidelity facilities, such as NASA's Glenn Extreme Environments Rig (GEER), are still required to reproduce coupled temperature, pressure, and atmospheric stresses for ground-based qualification [144]. In contrast, many newly emerging material-based sensors are still being evaluated in the simplified test chambers described in the previous chapter. This contrast highlights the need to move from isolated performance testing to multi-stressor evaluation with defined operating windows, setting the basis for the following discussion on lifetime preservation, robust sampling and packaging, and adaptive calibration strategies.

Furthermore, rapid warning capability should be evaluated as a deployment-level metric, rather than reduced to the intrinsic response time of the sensing material. Recent studies suggest two complementary approaches. The first is material- and device-level acceleration, in which shortened diffusion pathways, engineered interfaces, or suspended architectures amplify early optical or electrical responses. Representative examples include metal-polymer plasmonic nanomaterials that enable sub-second optical H_2 responses and fully suspended Pd nanowires that achieve an electrical response of approximately 0.6 s for H_2 detection [145,146]. The second is algorithm-assisted early prediction, in which transient response features are used to estimate gas concentration before the signal reaches full saturation. This approach has been demonstrated by vertical thermal-conduction sensor systems with neural-network prediction, achieving 0.4 s H_2 detection, and by integrated Pd-alloy leakage sensors with concentration-prediction algorithms, reaching 0.3 s concentration output [147,148]. These studies indicate that future harsh-environment gas sensors should be evaluated not only by steady-state sensitivity and stability but also by warning latency, transient-response reliability, and false-alarm resistance under application-specific operating conditions.

5.1. Stability and lifespan enhancement

Stability is the capacity of a sensor to keep its baseline, span, and response profile essentially unchanged under fixed conditions, with minimal and quantifiable drift. Reports commonly separate short-term stability over hours to days and long-term stability over weeks to months, noting drift as a relative change per unit time along with the recalibration interval [79]. A key challenge is that inadequate stability

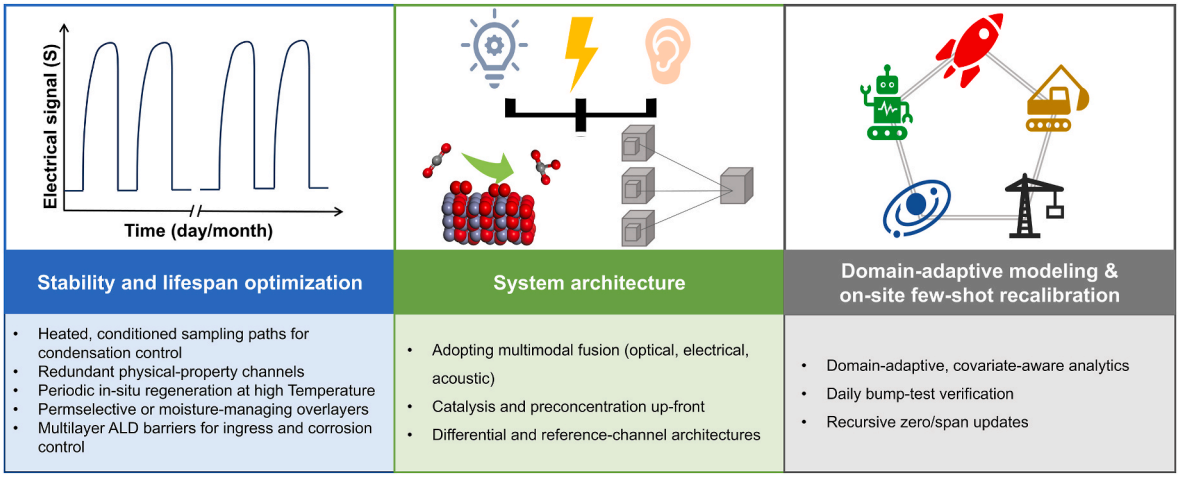

Fig. 9. Schematic diagram of gas detection stability issues under extreme conditions, solution strategies, and design guidance.

often results from multiple interconnected mechanisms. Temperature exposure and thermal cycling promote microstructural changes and diffusion of electrodes or dopants, especially in high-temperature stacks [54]. Chemical poisoning deactivates catalytic or electrode sites, with sulfur compounds and siloxanes in exhaust streams being well-documented causes [149]. Moisture can modify surface chemistry and charge transport, contributing to baseline drift in chemiresistive oxides [150]. Additionally, packaging and interconnects add new drift channels through thermo-mechanical stress, permeation, and corrosion, particularly when barrier layers are insufficient or chemically unstable [151]. Flow, pressure, and temperature transients also generate non-stationary transport, disrupting steady responses, especially in continuous field operation [152].

These mechanisms become more pronounced in harsh environments. High temperatures accelerate grain growth, phase transitions, and interdiffusion, while condensation and corrosive media thicken interfacial water films and open permeation paths, speeding up material aging and package failure. Fieldable practice is converging on a few measures that directly stop the main drift pathways through continuous monitoring. Heated and conditioned sampling paths that keep the transported gas above its dew point, along with good probe design and bias control, prevent condensation and wall losses in wet, corrosive streams and are now part of guidance for continuous emission monitoring systems and vendor practices. At the device and package level, multilayer barriers created by atomic layer deposition outperform single oxide layers by combining low water-vapor transmission with better chemical durability, such as Al_2O_3 paired with SiO_2, or ZrO_2 to reduce hydrolysis and corrosion [153,154]. These nanolaminates decrease ingress and keep interfaces stable over long campaigns.

When interferents, rather than permeation, dominate, thin permselective overlays like zeolites or MOF-derived films placed upstream of the sensitive layer shape transport and reduce cross-responses without significantly affecting kinetics. This approach has been validated from early zeolite capping of WO_3 and SnO_2 to modern membrane filter techniques [155,156]. In addition, inlet hardware resistant to droplet impact and particulate fouling, such as sintered-metal caps and flame-arrestor covers, protects the sensing head in hot and corrosive media and reduces maintenance needs.

At the material and transducer levels, several stability-oriented strategies are emerging. High-temperature acoustic transducers on langasite with high-melting-point multilayer electrodes and temperature-strain decoupling have demonstrated reliable operation at 500°C, with wireless temperature readout reported up to 1200°C, making them suitable for passive nodes in furnaces and turbines [157,158]. Entropy-stabilized oxides are starting to produce single-phase chemiresistors that resist coarsening and phase separation while maintaining response, indicating better long-term stability at high temperatures [159,160].

Facet-controlled metal oxides offer a complementary, interface-level strategy by exposing undercoordinated, high-energy surface sites that can enhance adsorption, oxygen activation, and surface-barrier modulation [161,162]. However, these facets also introduce an activity-stability trade-off in harsh environments because they are susceptible to surface reconstruction, hydroxylation, and sintering. Their practical use, therefore, requires stabilization through dopant anchoring, conformal protective shells, or heterointerface confinement, together with long-term drift and thermal/humidity-cycling validation [30,32]. Anti-condensation surface treatments at the inlet, using durable superhydrophobic or photothermal coatings, can delay film formation and fouling during rapid weather or load changes, smoothing the baseline over daily cycles [163]. On the operational side, temperature-programmed sensing captures richer, kinetic-based features that help distinguish target signals from interferents and aging effects, and is increasingly combined with lightweight on-edge models [164]. Long-term stability is further enhanced by treating deployment as a domain-shift problem, with scheduled bump or span checks supporting semi-supervised, active learning, or transfer learning approaches that have proven effective in reducing drift across multi-month datasets from electronic-nose platforms [165,166]. Overall, gas sensor stability in harsh environments depends on a finely tuned system across materials, packaging, sampling, and data calibration rather than a single fix.

5.2. System architecture

Because harsh environments can cause sensing failure, performance can be safeguarded by adopting multimodal fusion (optical, electrical, acoustic), catalysis, and upfront preconcentration, and differential and reference-channel architectures. By preparing the sample before measurement, sensing with complementary modalities, and stabilizing readout via differential referencing, a practical route to sustained selectivity, accuracy, and uptime in harsh deployments can be achieved. Recent nanocomposite-enabled chemical sensors also offer useful architectural references for harsh-environment gas-sensing systems. Self-powered biochemical sensors based on metal-air batteries illustrate routes to prolonged chemical monitoring without a continuous external power supply [167]. Programmable ferroelectric nanocomposites and self-powered sensory textiles further show that polymer-filler coupling, aligned composite structures, and textile-level integration can support low-power, flexible, and multifunctional sensing platforms [168,169].

Harsh environments weaken reliability when only a single sensing principle is used. Combining different transducers, such as MOS or transistor channels, with MIR spectroscopy and surface acoustic wave (SAW)/QCM mass sensors offers complementary selectivity and provides orthogonal failure modes. Field studies and reviews show that multimodal pipelines integrated with machine-learning fusion enhance classification, quantification, and anomaly detection for industrial gas monitoring and leak detection [170]. SAW/QCM devices coated with two-dimensional materials demonstrate high mass sensitivity at room temperature and remain effective in dusty or humid conditions [171,172]. Optical channels deliver long-lasting references with low drift and high resistance to humidity, stabilizing systems that include chemiresistors susceptible to drift [173]. In catalysis and preconcentration, MEMS micro-preconcentrators that periodically trap and thermally desorb analytes boost signal-to-noise ratio and lower LoDs for trace VOCs in low-temperature or humid environments [174]. Catalytic or size-selective filters placed before the sensing layer alter or remove interferents, enhancing selectivity and baseline stability in complex backgrounds [175]. Additionally, paired target-reference channels within the same flow and thermal environment suppress common-mode disturbances and monitor sensor health through residual analysis. Dual-channel NDIR CO_2 sensors integrating a MEMS emitter, thermopile detectors, and a compact optical cell demonstrate improved stability, humidity tolerance, and sensitivity while reducing size and power consumption [173,176].

5.3. Domain-adaptive modeling and on-site few-shot recalibration

Beyond material stability and system engineering, a highly practical approach for harsh-environment gas detection is to implement operational, domain-adaptive analytics with routine bump checks and a standard temperature-modulated sensing protocol. This approach should be understood as a data-level extension of the material and device strategies discussed above, because harsh environments first perturb the sensing interface and device readout before these changes manifest as variations in sensor data. Temperature cycling, humidity fluctuations, pressure or flow changes, vibration, and background gas variations can alter adsorption-desorption kinetics, surface reaction rates, charge or ion transport, optical path stability, and baseline signals. As a result, the response distribution observed during field deployment may deviate from laboratory calibration data, leading to data drift or domain shift.

Environmental covariates such as temperature, humidity, pressure,

flow, and vibration should therefore be recorded together with sensor signals, and online, transfer, or active-learning models can be used to reduce long-term drift and site-to-site shifts. Studies on electronic nose systems show that domain adaptation and online learning significantly enhance robustness to drift [165,177]. Brief daily bump tests with challenge gases can verify gas access and alarm function. Additionally, lightweight recursive updates (e.g., Recursive Least Squares (RLS) can be used to recursive PCA, or partial least squares (PLS)) to continuously update the zero/span with a handful of labeled points, maintaining accuracy between scheduled calibrations without downtime [178].

Importantly, AI-based correction can compensate only for reversible or statistically learnable variations, including baseline drift, environmental cross-sensitivity, sensor-to-sensor variation, gas classification and concentration prediction, and calibration transfer [166,178,179]. It cannot recover valid signals after irreversible material degradation, poisoning, corrosion, delamination, optical-window contamination, or packaging failure. These failure modes still require stable sensing materials, protective interfaces, conditioned sampling paths, reference channels, and robust device packaging. Therefore, domain-adaptive modeling should be integrated with material stabilization and device architecture to preserve valid sensing signals and improve calibration transferability and long-term interpretability.

6. Conclusion

Recent advances have improved harsh-environment gas sensing, but field reliability remains limited by coupled material, device, and calibration failures. This review systematically examines current engineering methods, ongoing challenges, and potential applications of gas sensors designed for operation in high- and low-temperature, high-humidity, and vacuum environments. Environments with high temperatures, such as combustion chambers, industrial furnaces, and aerospace applications, require sensor materials that maintain chemical and structural stability under thermal stress. Promising options like wide-bandgap semiconductors and thermally stable metal oxides have shown potential. However, issues such as sensor drift and long-term material degradation remain unresolved, necessitating further improvements in material design and stabilization techniques. Low-temperature environments, including cryogenics, polar regions, and space exploration, impose distinct challenges due to sluggish gas-surface reactions and the risk of condensation or freezing. Integrated microheaters, catalytic enhancements, and thermally robust packaging have been developed to mitigate these effects. However, optimizing energy efficiency and long-term reliability under prolonged low-temperature exposure remains a key challenge. High-humidity conditions, commonly encountered in environmental monitoring and precision agriculture, pose challenges for gas sensors due to moisture interference, competitive adsorption, and material degradation. Hydrophobic surface modification and signal-compensation strategies have mitigated some of these effects. However, maintaining consistent sensor performance over extended periods remains difficult. In vacuum environments, typical in space exploration and semiconductor manufacturing, traditional sensing methods are challenged by very low gas densities. Optical, spectroscopic, and field-ionization methods reduce reliance on surface adsorption and are attractive for low-density gas environments. Still, integrating these systems into compact, energy-efficient platforms remains a major challenge.

Future advancements in gas-sensing technologies are expected to stem from integrating emerging materials, adaptive device architectures, and advanced signal-processing strategies. Harsh-environment gas sensors should therefore move toward multifunctional, miniaturized, and self-sustaining platforms through material-device-system co-design. At the material level, the most actionable strategy is to stabilize the sensing interface where gas access, surface reaction, and signal drift originate. Entropy-stabilized oxides, ALD-based multilayer barriers, permselective zeolite or MOF-derived films, and anti-condensation coatings offer practical routes to suppress coarsening, permeation, fouling, and cross-response while preserving active sites. At the device level, robust architectures should condition the gas before sensing and compare the target response with an internal reference. MEMS micropreconcentrators, catalytic or size-selective filters, target-reference channels, and dual-channel NDIR designs therefore provide effective routes to improve selectivity, baseline stability, humidity robustness, and operational reliability. At the system level, long-term accuracy should be maintained by treating field deployment as a domain-shift problem. Temperature-programmed operation, environmental covariate inputs, online or transfer learning, and adaptive zero/span updates offer practical routes for drift correction, domain adaptation, and on-site recalibration. Such interdisciplinary efforts will expand sensing capabilities across aerospace, geothermal energy, deep-sea exploration, and planetary research. Overall, the major barrier to harsh-environment gas sensing is not optimizing sensor response under isolated laboratory stressors, but rather translating that response into reliable operation under simultaneous, interacting extremes. Future progress will depend on field-relevant validation that bridges laboratory performance and continuous monitoring in real extreme-service environments.

CRediT authorship contribution statement

Kewei Liu: Writing – original draft. **Yiwen Zhou:** Writing – review & editing. **Yongbin Qin:** Writing – review & editing. **Carla Bittencourt:** Writing – review & editing. **Zichen Zheng:** Conceptualization, Funding acquisition, Supervision, Writing – original draft.

Declaration of competing interest

The authors declare that they have no known competing financial interests or personal relationships that could have appeared to influence the work reported in this paper.

Acknowledgments

This work was supported by the China Scholarship Council (Grant No. 202308320445), Postgraduate Research and Practice Innovation Program of Jiangsu Province of China (Grant No. KYCX23_3551), and China Scholarship Council (Grant No. 202208320269). C.B. is a research associate of the FNRS-Belgium.

Data availability

Data will be made available on request.

References

[1] A.R. Santos, M.S. Gilmore, J.P. Greenwood, L.M. Nakley, K. Phillips, T. Kremic, X. Lopez, Experimental weathering of rocks and minerals at Venus conditions in the Glenn Extreme Environments Rig (GEER), J. Geophys. Res. Planets 128 (2023), https://doi.org/10.1029/2022JE007423 e2022JE007423.

[2] J. Feng, J. Geng, H. Zhang, C. Yang, L. Zou, B. Chi, J. Pu, Insight into the thermal hydrolysis behaviors of 5Y-TZP based oxygen sensor: effect of grain size dependent T-M phase transformation and residual stress, Sensor. Actuator. B Chem. 374 (2023) 132845, https://doi.org/10.1016/j.snb.2022.132845.

[3] L. Klose, C. Kleint, W. Bach, A. Diehl, F. Wilckens, C. Peters, H. Strauss, K. Haase, A. Koschinsky, Hydrothermal activity and associated subsurface processes at Niuatahi rear-arc volcano, North East Lau Basin, SW Pacific: implications from trace elements and stable isotope systematics in vent fluids, Geochem. Cosmochim. Acta 332 (2022) 103–123, https://doi.org/10.1016/j.gca.2022.06.023.

[4] T. Barreyre, J.-A. Olive, D.J. Fornari, J.M. McDermott, R. Parnell-Turner, K. Moutard, J.-N. Wu, M. Marjanović, Hydrothermal vent temperatures track magmatic inflation and forecast eruptions at the East Pacific Rise, 9°50'N 122 (2025) e2510245122, https://doi.org/10.1073/pnas.2510245122.

[5] H. Kappert, S. Schopferer, N. Saeidi, S. Ziesche, A. Olowinsky, F. Naumann, M. Jaegle, M. Spanier, Sensor systems for extremely harsh environments, Sensors and Measuring Systems; 21th ITG/GMA-Symposium, Nuremberg, Germany (2022) 1–3.

[6] P. Najafi, A. Ghaemi, Chemiresistor gas sensors: design, Challenges, and Strategies: a comprehensive review, Chem. Eng. J. 498 (2024) 154999, https://doi.org/10.1016/j.cej.2024.154999.

[7] I. del Castillo-Velilla, A. Sousaraei, I. Romero-Muñiz, C. Castillo-Blas, A.S. J. Méndez, F.E. Oropeza, V.A. de la Peña O'Shea, J. Cabanillas-González, A. Mavrandonakis, A.E. Platero-Prats, Synergistic binding sites in a metal-organic framework for the optical sensing of nitrogen dioxide, Nat. Commun. 14 (2023) 2506, https://doi.org/10.1038/s41467-023-38170-9.

[8] J. Li, S. Xie, W. Zhu, W. Di, L. Gong, Self-powered ammonia gas sensor based on Ta_2O_5/Nb_2AlC nanocomposites for environmental monitoring in vegetable greenhouses, J. Environ. Chem. Eng. 13 (2025) 115294, https://doi.org/10.1016/j.jece.2024.115294.

[9] M. Ma, Z. Li, W. Zhu, M. Ju, L. Gong, Self-powered ammonia gas sensor based on $Ga_2O_3/Mo_2Ti_2AlC_3$ nanocomposite material for environmental monitoring in chicken farms, Chem. Eng. J. 510 (2025) 161722, https://doi.org/10.1016/j.cej.2025.161722.

[10] L. Wang, J. Song, C. Yu, Recent progress on mass-sensitive gas sensors for environmental and industrial applications, Measurement 249 (2025) 117039, https://doi.org/10.1016/j.measurement.2025.117039.

[11] H. Wang, Y. Zhao, Z. Yuan, H. Ji, F. Meng, Multiscale bidirectional temporal convolutional framework for industrial ketone organic solvent detection based on semiconductor gas sensor, IEEE Trans. Ind. Electron. 71 (2024) 16772–16782, https://doi.org/10.1109/TIE.2024.3384526.

[12] O.E. Aina, N. Zine, G. Raffin, N. Jaffrezic-Renault, A. Elaissari, A. Errachid, Integrated breath analysis technologies: current advances and future prospects, TrAC, Trends Anal. Chem. 181 (2024) 118048, https://doi.org/10.1016/j.trac.2024.118048.

[13] Y. Li, X. Wei, Y. Zhou, J. Wang, R. You, Research progress of electronic nose technology in exhaled breath disease analysis, Microsyst. Nanoeng. 9 (2023) 129, https://doi.org/10.1038/s41378-023-00594-0.

[14] K. Liu, Z. Zheng, Y. Zhou, C. Bittencourt, M. Debliquy, Q. Liu, C. Zhang, Heterovalent-doping-induced ultrasensitive and highly exclusive ethylene sensor: application to crop quality inspection, Chem. Eng. J. 508 (2025) 161075, https://doi.org/10.1016/j.cej.2025.161075.

[15] A. Ali, A.S. Mansol, A.A. Khan, K. Muthoosamy, Y. Siddiqui, Electronic nose as a tool for early detection of diseases and quality monitoring in fresh postharvest produce: a comprehensive review, Compr. Rev. Food Sci. Food Saf. 22 (2023) 2408–2432, https://doi.org/10.1111/1541-4337.13151.

[16] T. Elias Abi-Ramia Silva, F. Burisch, A.T. Güntner, Gas sensing for space: health and environmental monitoring, TrAC, Trends Anal. Chem. 177 (2024) 117790, https://doi.org/10.1016/j.trac.2024.117790.

[17] K. Bay, E. Celik, Synthesis and characterization of Al-Doped SnO_2 semiconducting thin films on glass substrate by sol–gel technique for gas sensors in aerospace applications, Arabian J. Sci. Eng. 50 (2025) 3987–4005, https://doi.org/10.1007/s13369-024-09416-5.

[18] B. Zong, S. Wu, Y. Yang, Q. Li, T. Tao, S. Mao, Smart gas sensors: recent developments and future prospective, Nano-Micro Lett. 17 (2024) 54, https://doi.org/10.1007/s40820-024-01543-w.

[19] Gas Sensor Market Size & Trends Analysis Report By Product, By type, by technology, by end-use, by Region, and segment forecasts, 2024 - 2030. https://www.grandviewresearch.com/industry-analysis/gas-sensors-market, 2024.

[20] Gas sensor market size, share & analysis report, 2024-2032. https://www.gminsights.com/industry-analysis/gas-sensors-market-size, 2024.

[21] A. Hakeem Anwer, M. Saadaoui, A.T. Mohamed, N. Ahmad, A. Benamor, State-of-the-Art advances and challenges in wearable gas sensors for emerging applications: innovations and future prospects, Chem. Eng. J. 502 (2024) 157899, https://doi.org/10.1016/j.cej.2024.157899.

[22] X. Chen, W. Zheng, X. Li, K. Chen, Y. Yuan, Y. Liu, T. Yang, Y. Ye, W. Liang, W. Dong, W. Zhang, S. Jiang, Y. Fu, W. Luo, Outer space H_2S detection: cuo-based thin film gas sensors powered by UV-LED in vacuum, Chem. Eng. J. 505 (2025) 159681, https://doi.org/10.1016/j.cej.2025.159681.

[23] S. Yu, X. Jia, J. Zhang, W. Yang, H. Song, Recent advances in different materials for moisture resistance of metal oxide-based gas sensors: a review, Chem. Eng. J. 505 (2025) 159639, https://doi.org/10.1016/j.cej.2025.159639.

[24] C. Zhang, T. Wang, G. Zhang, R. Gao, C. Gao, Z. Wang, F. Xuan, Rational design and fabrication of MEMS gas sensors with long-term stability: a comprehensive review, Adv. Sci. 12 (2025) e11555, https://doi.org/10.1002/advs.202511555.

[25] K. Liu, Z. Zheng, M. Debliquy, C. Zhang, Highly-sensitive volatile organic compounds evaluation by three-dimensional $ZnFe_2O_4/ZnSnO_3$ heterostructures and their predictive grain quality monitoring, Chem. Eng. J. 453 (2023) 139824, https://doi.org/10.1016/j.cej.2022.139824.

[26] J. Li, W. Si, L. Shi, R. Gao, Q. Li, W. An, Z. Zhao, L. Zhang, N. Bai, X. Zou, G.-D. Li, Essential role of lattice oxygen in hydrogen sensing reaction, Nat. Commun. 15 (2024) 2998, https://doi.org/10.1038/s41467-024-47078-x.

[27] S.P. Linto Sibi, M. Rajkumar, M. Manoharan, J. Mobika, V. Nithya Priya, R. T. Rajendra Kumar, Humidity activated ultra-selective room temperature gas sensor based on W doped MoS_2/RGO composites for trace level ammonia detection, Anal. Chim. Acta 1287 (2024) 342075, https://doi.org/10.1016/j.aca.2023.342075.

[28] A. Marikutsa, M. Rumyantseva, E.A. Konstantinova, A. Gaskov, The key role of active sites in the development of selective metal oxide sensor materials, Sensors 21 (2021), https://doi.org/10.3390/s21072554.

[29] Liquid hydrogen delivery. https://www.energy.gov/eere/fuelcells/liquid-hydrogen-delivery.

[30] E.B. Kim, K.Y. Shin, W. Oum, S. Moon, A. Mirzaei, S.S. Kim, H.W. Kim, Optimization of Al_2O_3 shell thickness on SnO_2 nanowires for realization of sensitive and selective H_2 sensing, Sensor. Actuator. B Chem. 426 (2025) 137021, https://doi.org/10.1016/j.snb.2024.137021.

[31] Q. Zhang, Y. Liu, H. Li, J. Wang, Y. Wang, F. Cheng, H. Han, P. Zhang, A review of SiC sensor applications in high-temperature and radiation extreme environments, Sensors 24 (2024), https://doi.org/10.3390/s24237731.

[32] Y.H. Kim, H. Jeong, B.-R. Won, H. Jeon, C.-h. Park, D. Park, Y. Kim, S. Lee, J.-h. Myung, Nanoparticle exsolution on perovskite oxides: insights into mechanism, characteristics and novel strategies, Nano-Micro Lett. 16 (2023) 33, https://doi.org/10.1007/s40820-023-01258-4.

[33] X. Bévenot, A. Trouillet, C. Veillas, H. Gagnaire, M. Clément, Hydrogen leak detection using an optical fibre sensor for aerospace applications, Sensor. Actuator. B Chem. 67 (2000) 57–67, https://doi.org/10.1016/S0925-4005(00)00407-X.

[34] T. Ramos Canabarra dos Santos, M. de Jesus Bassi, M. Muller de França, J. K. Majewski, M.V.W. Barcote, A.E.P. Stanislawczuk, L.S. Roman, Gas sensor based on highly effective slot-die printed PEDOT:PSS@ZnO hybrid nanocomposite for methanol detection, ACS Appl. Mater. Interfaces 17 (2025) 13065–13073, https://doi.org/10.1021/acsami.4c03131.

[35] Q. Wu, Y. Yuan, M. Jiao, X. Wang, W. Liu, X. Bu, C. Han, X. Li, X. Wang, Hydrogen-bond acidic organic compound-sensitized ionic gel for dimethyl methylphosphonate detection, Sensor. Actuator. B Chem. 391 (2023) 134068, https://doi.org/10.1016/j.snb.2023.134068.

[36] R. Sarabia-Riquelme, W.C. Schimpf, D.L. Kuhn, M.C. Weisenberger, Influence of relative humidity on the structure, swelling and electrical conductivity of PEDOT:PSS fibers, Synth. Met. 297 (2023) 117399, https://doi.org/10.1016/j.synthmet.2023.117399.

[37] G. Chen, J. Li, H. Zhu, Y. Wang, H. Ji, F. Meng, Optical fiber gas sensor with multi-parameter sensing and environmental anti-interference performance, J. Ind. Inf. Integr. 38 (2024) 100565, https://doi.org/10.1016/j.jii.2024.100565.

[38] M.F. Haque, S. Park, D. Yang, Gas sensors in harsh environments: challenges and advances in high temperature, high humidity, radiative and corrosive conditions, J. Sci. Adv. Mater. Devices 10 (2025) 101049, https://doi.org/10.1016/j.jsamd.2025.101049.

[39] J. Wei, M. Zhao, C. Wang, J. Wang, J.-M. Ye, Y.-C. Wei, Z.-Y. Li, R. Zhao, G.-Z. Liu, Y.-H. Geng, R. Wang, H.-D. Xiao, Y. Li, C.-Y. Li, Z.-Q. Gao, J. Gao, Vacuum based gas sensing material characterization System for precise and simultaneous measurement of optical and electrical responses, Sensors 22 (2022), https://doi.org/10.3390/s22031014.

[40] Z. Du, X. Zhang, B. Xue, Z. Luan, J. Yan, The applications of the *in situ* laser spectroscopy to the deep-sea cold seep and hydrothermal vent system, Solid Earth Sci. 5 (2020) 153–168, https://doi.org/10.1016/j.sesci.2020.06.001.

[41] A. Sharma, S.B. Eadi, H. Noothalapati, M. Otyepka, H.-D. Lee, K. Jayaramulu, Porous materials as effective chemiresistive gas sensors, Chem. Soc. Rev. 53 (2024) 2530–2577, https://doi.org/10.1039/D2CS00761D.

[42] P.M. Bulemo, D.-H. Kim, H. Shin, H.-J. Cho, W.-T. Koo, S.-J. Choi, C. Park, J. Ahn, A.T. Güntner, R.M. Penner, I.-D. Kim, Selectivity in chemiresistive gas sensors: strategies and challenges, Chem. Rev. 125 (2025) 4111–4183, https://doi.org/10.1021/acs.chemrev.4c00592.

[43] L. Zhang, M. Zhou, F. Meng, J. Bai, D. Wang, M. Tang, Z. Wu, Recent advances in chemiresistive gas sensor for acetone detection: focus on room temperature, TrAC, Trends Anal. Chem. 187 (2025) 118213, https://doi.org/10.1016/j.trac.2025.118213.

[44] J.H. Bang, A. Mirzaei, M.S. Choi, S. Han, H.Y. Lee, S.S. Kim, H.W. Kim, Decoration of multi-walled carbon nanotubes with CuO/Cu_2O nanoparticles for selective sensing of H_2S gas, Sensor. Actuator. B Chem. 344 (2021) 130176, https://doi.org/10.1016/j.snb.2021.130176.

[45] C. Montoro, J.-Y. Kim, A. Mirzaei, J.-H. Lee, S. Sayegh, E. Makhoul, I. Iatsunskyi, E. Coy, M. Bechelany, H.W. Kim, S.S. Kim, MOF-derived metal oxide (Cu, Ni, Zn) gas sensors with excellent selectivity towards H_2S, CO and H_2 gases, Compos. B Eng. 283 (2024) 111637, https://doi.org/10.1016/j.compositesb.2024.111637.

[46] M. Sik Choi, J. Ahn, M. Young Kim, A. Mirzaei, S.-M. Choi, D. Won Chun, C. Jin, K. Hyoung Lee, Changes in the crystal structure of SnO_2 nanoparticles and improved H_2S gas-sensing characteristics by Al doping, Appl. Surf. Sci. 565 (2021) 150493, https://doi.org/10.1016/j.apsusc.2021.150493.

[47] K. Liu, Z. Zheng, Y. Zhou, C. Bittencourt, M. Debliquy, C. Zhang, Probing the challenge of P-Type semiconductors in long-chain VOC detection: 3D micro-flower zinc cobaltate heterojunction sensors, Adv. Sci. 12 (2025) e02646, https://doi.org/10.1002/advs.202502646.

[48] K. Kim, P.G. Choi, T. Itoh, Y. Masuda, Effect of oxygen vacancy sites in exposed crystal facet on the gas sensing performance of ZnO nanomaterial, J. Am. Ceram. Soc. 105 (2022) 2150–2160, https://doi.org/10.1111/jace.18240.

[49] S.M. Majhi, S.T. Navale, A. Mirzaei, H.W. Kim, S.S. Kim, Strategies to boost chemiresistive sensing performance of In_2O_3-based gas sensors: an overview, Inorg. Chem. Front. 10 (2023) 3428–3467, https://doi.org/10.1039/d3qi00099k.

[50] C. Chen, C. Ren, S. Yang, W. Li, G. Xie, H. Yuan, J. Yang, Y. Su, Voice-driven self-powered ethanol sensor for speech recognition and drunk driving detection, Sensor. Actuator. B Chem. 447 (2026) 138869, https://doi.org/10.1016/j.snb.2025.138869.

[51] W. Li, G. Xie, X. Huo, L. Que, H. Tai, Y. Jiang, Y. Su, Piezoelectric composites for gas sensing: evolution of sensing and transduction designs, J. Mater. Chem. C 13 (2025) 13582–13606, https://doi.org/10.1039/d5tc01383f.

[52] J. Li, G. Xie, L. Dai, M. Yang, Y. Su, Rapid and highly selective dopamine sensing with $CuInSe_2$-Modified nanocomposite, J. Compos. Sci. 9 (2025) 123, https://doi.org/10.3390/jcs9030123.

[53] T. Ritter, J. Zosel, U. Guth, Solid electrolyte gas sensors based on mixed potential principle – a review, Sensor. Actuator. B Chem. 382 (2023) 133508, https://doi.org/10.1016/j.snb.2023.133508.

[54] S. Halley, K.P. Ramaiyan, L.-k. Tsui, F. Garzon, A review of zirconia oxygen, NO_x, and mixed potential gas sensors – history and current trends, Sensor. Actuator. B Chem. 370 (2022) 132363, https://doi.org/10.1016/j.snb.2022.132363.

[55] S. Lv, T. Gu, Q. Pu, B. Wang, X. Jia, P. Sun, L. Wang, F. Liu, G. Lu, Integrated mixed potential gas sensor with efficient structure for discriminative volatile organic compounds detection, Adv. Sci. 11 (2024) 2405124, https://doi.org/10.1002/advs.202405124.

[56] J.W. Fergus, Solid electrolyte based sensors for the measurement of CO and hydrocarbon gases, Sensor. Actuator. B Chem. 122 (2007) 683–693, https://doi.org/10.1016/j.snb.2006.06.024.

[57] E. Gorbova, F. Tzorbatzoglou, C. Molochas, D. Chloros, A. Demin, P. Tsiakaras, Fundamentals and principles of solid-state electrochemical sensors for high temperature gas detection, Catalysts 12 (2022) 1, https://doi.org/10.3390/catal12010001.

[58] J. Hodgkinson, R.P. Tatam, Optical gas sensing: a review, Meas. Sci. Technol. 24 (2013) 012004, https://doi.org/10.1088/0957-0233/24/1/012004.

[59] C.J. Mitchell, T. Hu, S. Sun, C.J. Stirling, M. Nedeljkovic, A.C. Peacock, G.T. Reed, G.Z. Mashanovich, D.J. Rowe, Mid-infrared silicon photonics: from benchtop to real-world applications, APL Photonics 9 (2024) 080901, https://doi.org/10.1063/5.0222890.

[60] X. Tan, H. Zhang, J. Li, H. Wan, Q. Guo, H. Zhu, H. Liu, F. Yi, Non-dispersive infrared multi-gas sensing via nanoantenna integrated narrowband detectors, Nat. Commun. 11 (2020) 5245, https://doi.org/10.1038/s41467-020-19085-1.

[61] P.A. Mosier-Boss, Review of SERS substrates for chemical sensing, Nanomaterials 7 (2017), https://doi.org/10.3390/nano7060142.

[62] Z. Li, J.R. Askim, K.S. Suslick, The optoelectronic nose: colorimetric and fluorometric sensor arrays, Chem. Rev. 119 (2019) 231–292, https://doi.org/10.1021/acs.chemrev.8b00226.

[63] M.A. Butt, M. Juchniewicz, M. Słowikowski, Ł. Kozłowski, R. Piramidowicz, Mid-Infrared photonic sensors: exploring fundamentals, advanced materials, and cutting-edge applications, Sensors 25 (2025), https://doi.org/10.3390/s25041102.

[64] Y. Liu, Y. He, M. Hu, B. Chen, Z. Xu, L. Yao, X. Wang, R. Kan, Cavity ring-down spectroscopy with a laser frequency stabilized and locked to a reference target gas absorption for drift-free accurate gas sensing measurements, Volume 11 - 2023, https://doi.org/10.3389/fphy.2023.1238869, 2023.

[65] M. Xu, B. Peng, X. Zhu, Y. Guo, Multi-Gas Detection System based on non-dispersive infrared (NDIR) spectral technology, Sensors 22 (2022), https://doi.org/10.3390/s22030836.

[66] T.-V. Dinh, I.-Y. Choi, Y.-S. Son, J.-C. Kim, A review on non-dispersive infrared gas sensors: improvement of sensor detection limit and interference correction, Sensor. Actuator. B Chem. 231 (2016) 529–538, https://doi.org/10.1016/j.snb.2016.03.040.

[67] Y. Cui, K. Chang, Q. Wang, Y. Zhao, Advances of surface-enhanced Raman scattering in gas sensing, Coord. Chem. Rev. 524 (2025) 216320, https://doi.org/10.1016/j.ccr.2024.216320.

[68] A. Fernández-Lodeiro, M. Constantinou, C. Panteli, A. Agapiou, C. Andreou, Breath analysis via surface Enhanced Raman spectroscopy, ACS Sens. 10 (2025) 602–621, https://doi.org/10.1021/acssensors.4c02685.

[69] S.H. Cho, J.M. Suh, T.H. Eom, T. Kim, H.W. Jang, Colorimetric sensors for toxic and hazardous gas detection: a review, Electron. Mater. Lett. 17 (2021) 1–17, https://doi.org/10.1007/s13391-020-00254-9.

[70] A. Mujahid, A. Afzal, F.L. Dickert, An overview of high frequency acoustic Sensors—QCMs, SAWs and FBARs—Chemical and biochemical applications, Sensors 19 (2019) 4395, https://doi.org/10.3390/s19204395.

[71] I. Banga, A. Paul, D.C. Poudyal, S. Muthukumar, S. Prasad, Recent advances in gas detection methodologies with a special focus on environmental sensing and health monitoring applications—a critical review, ACS Sens. 8 (2023) 3307–3319, https://doi.org/10.1021/acssensors.3c00959.

[72] M. Wei-Hao Li, A. Ghosh, A. Venkatasubramanian, R. Sharma, X. Huang, X. Fan, High-Sensitivity micro-gas chromatograph–photoionization detector for trace vapor detection, ACS Sens. 6 (2021) 2348–2355, https://doi.org/10.1021/acssensors.1c00482.

[73] Y. Liu, J. Parisi, X. Sun, Y. Lei, Solid-state gas sensors for high temperature applications – a review, J. Mater. Chem. A 2 (2014) 9919–9943, https://doi.org/10.1039/c3ta15008a.

[74] Y. Wang, Y. Zhou, Recent progress on anti-humidity strategies of chemiresistive gas sensors, Materials 15 (2022) 8728, https://doi.org/10.3390/ma15248728.

[75] Y. Zhao, Y. Liu, B. Han, M. Wang, Q. Wang, Y.-n. Zhang, Fiber optic volatile organic compound gas sensors: a review, Coord. Chem. Rev. 493 (2023) 215297, https://doi.org/10.1016/j.ccr.2023.215297.

[76] J. Wang, H. Shen, Y. Xia, S. Komarneni, Light-activated room-temperature gas sensors based on metal oxide nanostructures: a review on recent advances, Ceram. Int. 47 (2021) 7353–7368, https://doi.org/10.1016/j.ceramint.2020.11.187.

[77] S.M. Majhi, A. Mirzaei, H.W. Kim, S.S. Kim, T.W. Kim, Recent advances in energy-saving chemiresistive gas sensors: a review, Nano Energy 79 (2021) 105369, https://doi.org/10.1016/j.nanoen.2020.105369.

[78] R. Kumar, X. Liu, J. Zhang, M. Kumar, Room-Temperature gas sensors under photoactivation: from metal oxides to 2D materials, Nano-Micro Lett. 12 (2020) 164, https://doi.org/10.1007/s40820-020-00503-4.

[79] H. Chai, Z. Zheng, K. Liu, J. Xu, K. Wu, Y. Luo, H. Liao, M. Debliquy, C. Zhang, Stability of metal oxide semiconductor gas sensors: a review, IEEE Sens. J. 22 (2022) 5470–5481, https://doi.org/10.1109/JSEN.2022.3148264.

[80] V.K. Khanna, Humidity and Contamination Effects on Electronics, Extreme-Temperature and Harsh-Environment Electronics, second ed., IOP Publishing, 2023, 15-1-15-12.

[81] V.K. Khanna, Extreme-Temperature and harsh-environment electronics. Physics, Technology and Applications, second ed., IOP Publishing, 2023.

[82] J. Li, E. Na, X. Liang, Q. Liang, M. Fan, H. Chen, G.-D. Li, X. Zou, Surface oxygen chemistry of metal oxide semiconductors for gas-sensing applications, Inorg. Chem. Front. 11 (2024) 8602–8626, https://doi.org/10.1039/d4qi02385d.

[83] A. Staerz, U. Weimar, N. Barsan, Current state of knowledge on the metal oxide based gas sensing mechanism, Sensor. Actuator. B Chem. 358 (2022) 131531, https://doi.org/10.1016/j.snb.2022.131531.

[84] C. Wang, L. Yin, L. Zhang, D. Xiang, R. Gao, Metal oxide gas sensors: sensitivity and influencing factors, Sensors 10 (2010) 2088–2106, https://doi.org/10.3390/s100302088.

[85] E. Comini, G. Faglia, G. Sberveglieri, UV light activation of tin oxide thin films for NO_2 sensing at low temperatures, Sensor. Actuator. B Chem. 78 (2001) 73–77, https://doi.org/10.1016/S0925-4005(01)00796-1.

[86] N.D. Chinh, N.D. Quang, H. Lee, T. Thi Hien, N.M. Hieu, D. Kim, C. Kim, D. Kim, NO gas sensing kinetics at room temperature under UV light irradiation of In_2O_3 nanostructures, Sci. Rep. 6 (2016) 35066, https://doi.org/10.1038/srep35066.

[87] N. Miura, T. Sato, S.A. Anggraini, H. Ikeda, S. Zhuiykov, A review of mixed-potential type zirconia-based gas sensors, Ionics 20 (2014) 901–925, https://doi.org/10.1007/s11581-014-1140-1.

[88] K. Liu, C. Ma, G. Ye, Y. Wang, W. Fan, Y. Cao, Advances in metal oxide semiconductor gas sensors for trace gas detection: from material fundamentals to device engineering, J. Alloys Compd. 1039 (2025) 183053, https://doi.org/10.1016/j.jallcom.2025.183053.

[89] L. Shu, X. Wang, D. Yan, L. Fan, W. Wu, The investigation of high-temperature SAW oxygen sensor based on ZnO films, Materials 12 (2019), https://doi.org/10.3390/ma12081235.

[90] S.G. Leonardi, A. Mirzaei, A. Bonavita, S. Santangelo, P. Frontera, F. Pantò, P. L. Antonucci, G. Neri, A comparison of the ethanol sensing properties of α-iron oxide nanostructures prepared via the sol–gel and electrospinning techniques, Nanotechnology 27 (2016) 075502, https://doi.org/10.1088/0957-4484/27/7/075502.

[91] A. Ghosh, S.B. Majumder, Modeling the sensing characteristics of chemi-resistive thin film semi-conducting gas sensors, Phys. Chem. Chem. Phys. 19 (2017) 23431–23443, https://doi.org/10.1039/C7CP04241H.

[92] Z. Ma, T. Fei, T. Zhang, An overview: sensors for low humidity detection, Sensor. Actuator. B Chem. 376 (2023) 133039, https://doi.org/10.1016/j.snb.2022.133039.

[93] J.-W. Yoon, J.-S. Kim, T.-H. Kim, Y.J. Hong, Y.C. Kang, J.-H. Lee, A new strategy for humidity independent oxide chemiresistors: dynamic self-refreshing of In_2O_3 sensing surface assisted by layer-by-layer coated CeO_2 nanoclusters, Small 12 (2016) 4229–4240, https://doi.org/10.1002/smll.201601507.

[94] A.V. Agrawal, A.Y. Polyakov, J. Eriksson, T.J. Antosiewicz, T.O. Shegai, Humidity-Enhanced NO_2 gas sensing using atomically sharp edges in Multilayer MoS_2, Small Struct. 6 (2025) 2400409, https://doi.org/10.1002/sstr.202400409.

[95] X. Chen, J. Hu, P. Chen, M. Yin, F. Meng, Y. Zhang, UV-light-assisted NO_2 gas sensor based on WS_2/PbS heterostructures with full recoverability and reliable anti-humidity ability, Sensor. Actuator. B Chem. 339 (2021) 129902, https://doi.org/10.1016/j.snb.2021.129902.

[96] M. Verma, G. Bahuguna, A. Saharan, S. Gaur, H. Haick, R. Gupta, Room temperature humidity tolerant xylene sensor using a Sn-SnO_2 nanocomposite, ACS Appl. Mater. Interfaces 15 (2023) 5512–5520, https://doi.org/10.1021/acsami.2c22417.

[97] T.-W. Kim, J.-W. Kim, S.-M. Lee, C.-O. Park, Humidity effects on the initial stabilization behavior of a solid electrochemical CO_2 sensor, Sensor. Actuator. B Chem. 295 (2019) 65–69, https://doi.org/10.1016/j.snb.2019.05.015.

[98] F. Souza, J. Fabius, S. Zhuang, J. Vonk, B. Celikkol, S. Gaitan, Modeling humidity and temperature effects on electrochemical gas sensors at low concentrations, in: 2024 IEEE International Instrumentation and Measurement Technology Conference (I2MTC), 2024, pp. 1–6.

[99] X. Pang, M.D. Shaw, A.C. Lewis, L.J. Carpenter, T. Batchellier, Electrochemical ozone sensors: a miniaturised alternative for ozone measurements in laboratory experiments and air-quality monitoring, Sensor. Actuator. B Chem. 240 (2017) 829–837, https://doi.org/10.1016/j.snb.2016.09.020.

[100] S. Pyo, K. Lee, T. Noh, E. Jo, J. Kim, Sensitivity enhancement in photoionization detector using microelectrodes with integrated 1D nanostructures, Sensor. Actuator. B Chem. 288 (2019) 618–624, https://doi.org/10.1016/j.snb.2019.03.045.

[101] C. Romero-Trigueros, M. Doval Miñarro, E. González Duperón, E. González Ferradás, Influence of sample temperature and environmental humidity on measurements of benzene in ambient air by transportable GC-PID, Atmos. Meas. Tech. 10 (2017) 4013–4022, https://doi.org/10.5194/amt-10-4013-2017.

[102] H. Bai, G. Shi, Gas sensors based on conducting polymers, Sensors 7 (2007) 267–307, https://doi.org/10.3390/s7030267.

[103] S. Gasso, J. Carrier, D. Radu, C.-Y. Lai, Novel gas sensing approach: ReS_2/Ti_3C_2Tx heterostructures for NH_3 detection in humid environments, ACS Sens. 9 (2024) 4788–4802, https://doi.org/10.1021/acssensors.4c01216.

[104] R. Radebaugh, About Cryogenics, 2002. https://trc.nist.gov/cryogenics/aboutCryogenics.html. (Accessed 6 July 2026).

[105] Z. Yuan, H. Schreuders, R. Dankelman, B. Dam, L.J. Bannenberg, Optical hydrogen sensing materials for applications at sub-zero temperatures, Adv. Funct. Mater. (2025) 2420087, https://doi.org/10.1002/adfm.202420087.
[106] W. Pi, X. Chen, M. Humayun, Y. Yuan, W. Dong, G. Zhang, B. Chen, Q. Fu, Z. Lu, H. Li, Z. Tang, W. Luo, Highly sensitive chemiresistive H_2S detection at subzero temperature over the Sb-Doped SnO_2@g-C_3N_4 heterojunctions under UV illumination, ACS Appl. Mater. Interfaces 15 (2023) 14979–14989, https://doi.org/10.1021/acsami.3c00213.
[107] P. Guo, X. He, X. An, X. Zhang, S. Liang, J. Zhang, Y. Fu, N-doped carbon dots/SnS_2 heterostructures for ultra-fast and sub-ppb-level detection of NO_2 in multiple environments, Chem. Eng. J. 500 (2024) 156882, https://doi.org/10.1016/j.cej.2024.156882.
[108] Leybold, The Fundamentals of Rough & Medium Vacuum. Leybold Global. https://www.leybold.com/en/knowledge/blog/rough-medium-vacuum. (Accessed 6 July 2026).
[109] N. Barsan, D. Koziej, U. Weimar, Metal oxide-based gas sensor research: how to? Sensor. Actuator. B Chem. 121 (2007) 18–35, https://doi.org/10.1016/j.snb.2006.09.047.
[110] S.-Y. Jeong, Y.K. Moon, J. Wang, J.-H. Lee, Exclusive detection of volatile aromatic hydrocarbons using bilayer oxide chemiresistors with catalytic overlayers, Nat. Commun. 14 (2023) 233, https://doi.org/10.1038/s41467-023-35916-3.
[111] G. Korotcenkov, Metal oxides for solid-state gas sensors: what determines our choice? Mater. Sci. Eng., B 139 (2007) 1–23, https://doi.org/10.1016/j.mseb.2007.01.044.
[112] G. Sberveglieri, Recent developments in semiconducting thin-film gas sensors, Sensor. Actuator. B Chem. 23 (1995) 103–109, https://doi.org/10.1016/0925-4005(94)01278-P.
[113] C.C. Wang, S.A. Akbar, M.J. Madou, Ceramic based resistive sensors, J. Electroceram. 2 (1998) 273–282, https://doi.org/10.1023/A:1009978607621.
[114] W. Pi, X. Chen, Q. Fu, Z. Lu, H. Li, Z. Tang, W. Luo, The gas-sensing performance of a core–shell SnO_2-based chemiresistive MEMS sensor for H_2S detection under vacuum, J. Mater. Chem. C 11 (2023) 12517–12524, https://doi.org/10.1039/D3TC01940C.
[115] F. Wang, S. Wang, Y. Liu, Z. Hu, S. Zhang, S. Ouyang, S. Ma, Z. Wu, Z. Zhao, M. Li, Y. Wu, L. Wang, C. Jia, J. Zhao, Enhanced air filtration and ammonia sensing with cellulose nanofibers-based triboelectric nanogenerators under harsh environments, Nano Energy 131 (2024) 110323, https://doi.org/10.1016/j.nanoen.2024.110323.
[116] C. Qin, Z. Wei, X. Zhao, J. Cao, Y. Wang, High-temperature hydrogen sensor based on MOFs-derived Mn-doped In_2O_3 hollow nanotubes, Int. J. Hydrogen Energy 78 (2024) 1024–1033, https://doi.org/10.1016/j.ijhydene.2024.06.371.
[117] H. Tae Won, L. Dae-Yun, L. Chil-Hyoung, High-Temperature stable NO_x sensor for exhaust gas monitoring in automobiles, J. Sens. Sci. Technol. 33 (2024) 439–447, https://doi.org/10.46670/JSST.2024.33.6.439.
[118] C. Heath, B. Pejcic, M.B. Myers, Block copolymer-coated ATR-FTIR spectroscopic sensors for monitoring hydrocarbons in aquatic environments at high temperature and pressure, ACS Appl. Polym. Mater. 1 (2019) 2149–2156, https://doi.org/10.1021/acsapm.9b00420.
[119] Z. Chen, Y. Liu, R. Liu, Y. Chen, H. Liu, X. Cheng, Response enhancement in high-temperature H_2S-Treated metal oxide gas sensors, ACS Sens. 9 (2024) 3979–3985, https://doi.org/10.1021/acssensors.4c00749.
[120] S. Mourya, A. Kumar, J. Jaiswal, G. Malik, B. Kumar, R. Chandra, Development of Pd-Pt functionalized high performance H_2 gas sensor based on silicon carbide coated porous silicon for extreme environment applications, Sensor. Actuator. B Chem. 283 (2019) 373–383, https://doi.org/10.1016/j.snb.2018.12.042.
[121] Z. Zheng, K. Liu, M. Debliquy, C. Zhang, Carbon functionalized cladding bismuth tungstate-based 3D twisted micro-flowers for benzaldehyde detection under ultraviolet light excitation, Sensor. Actuator. B Chem. 415 (2024) 135982, https://doi.org/10.1016/j.snb.2024.135982.
[122] Y. Yamazaki, T. Hitomi, C. Homma, T. Rungreungthanapol, M. Tanaka, K. Yamada, H. Hamasaki, Y. Sugizaki, A. Isobayashi, H. Tomizawa, M. Okochi, Y. Hayamizu, Enantioselective detection of gaseous odorants with peptide–graphene sensors operating in humid environments, ACS Appl. Mater. Interfaces 16 (2024) 18564–18573, https://doi.org/10.1021/acsami.4c01177.
[123] O. Wang, X. Zhang, J. Kong, H. Liu, Y. Zhao, B. An, J. Xu, X. Wang, Fabrication of 2D/3D organic-inorganic hybrid perovskite derived materials and its low temperature response to formaldehyde at high humidity, Sensor. Actuator. B Chem. 403 (2024) 134942, https://doi.org/10.1016/j.snb.2023.134942.
[124] Y. Je, S.-S. Chee, High-speed and sub-ppm detectable tellurene NO_2 chemiresistive room-temperature sensor under humidity environments, Electron. Mater. Lett. 21 (2025) 94–101, https://doi.org/10.1007/s13391-024-00520-0.
[125] Y. Wang, Z. Song, Y. Liu, Y. Chen, J. Li, L. Li, J. Yao, Methyl functionalization of trimesic acid in copper-based metal-organic framework for ammonia colorimetric sensing at high relative humidity, Chin. Chem. Lett. 35 (2024) 108779, https://doi.org/10.1016/j.cclet.2023.108779.
[126] M. Xu, Y. Xu, J. Tao, L. Wen, C. Zheng, Z. Yu, S. He, Development of a compact NDIR CO_2 gas sensor for harsh environments, Infrared Phys. Technol. 136 (2024) 105035, https://doi.org/10.1016/j.infrared.2023.105035.
[127] Q. Ding, Z. Zhou, H. Wang, Z. Wu, K. Tao, B.-R. Yang, X. Xie, J. Fu, J. Wu, Self-healable, recyclable, ultrastretchable, and high-performance NO_2 sensors based on an organohydrogel for room and sub-zero temperature and wireless operation, SmartMat 4 (2023) e1141, https://doi.org/10.1002/smm2.1141.
[128] N. Chakraborty, S. Mondal, Chemiresistive NH_3 detection at sub-zero temperatures by polypyrrole- loaded $Sn_{1-x}Sb_xO_2$ nanocubes, Mater. Horiz. 9 (2022) 1750–1762, https://doi.org/10.1039/D2MH00236A.
[129] G. Kyriakou, A. Stevens, D. Davis, R. Grant, M. Tikhov, R. Lambert, Amperometric/potentiometric hydrocarbon sensors: real world solutions for use in ultra high vacuum, J. Appl. Electrochem. 38 (2008) 1089–1096, https://doi.org/10.1007/s10800-008-9568-5.
[130] V. Snitka, D. Batiuskaite, I. Bruzaite, U. Lafont, Y. Butenko, C. Semprimoschnig, Surface-enhanced Raman scattering sensors for biomedical and molecular detection applications in space, CEAS Space Journal 13 (2021) 509–520, https://doi.org/10.1007/s12567-021-00356-6.
[131] A. Ghosh, C. Zhang, S.Q. Shi, H. Zhang, High-Temperature gas sensors for harsh environment applications: a review, CLEAN – soil, Air, Water 47 (2019) 1800491, https://doi.org/10.1002/clen.201800491.
[132] N. Samotaev, B. Podlepetsky, M. Mashinin, I. Ivanov, I. Obraztsov, K. Oblov, P. Dzhumaev, Thermal conductivity gas sensors for high-temperature applications, Micromachines 15 (2024), https://doi.org/10.3390/mi15010138.
[133] A. Mirzaei, S.G. Leonardi, G. Neri, Detection of hazardous volatile organic compounds (VOCs) by metal oxide nanostructures-based gas sensors: a review, Ceram. Int. 42 (2016) 15119–15141, https://doi.org/10.1016/j.ceramint.2016.06.145.
[134] S. Navazani, A. Shokuhfar, M. Hassanisadi, M. Askarieh, A. Di Carlo, A. Agresti, Facile synthesis of a SnO_2@rGO nanohybrid and optimization of its methane-sensing parameters, Talanta 181 (2018) 422–430, https://doi.org/10.1016/j.talanta.2018.01.015.
[135] X.-Y. Huang, K. Chen, W. Xie, Y. Li, F. Yang, Y. Deng, J. Li, F. Jiang, Y. Shu, L. Wu, W.-F. Xie, Y. Deng, Chemiresistive gas sensors based on highly permeable Sn-Doped bismuth subcarbonate microspheres: facile synthesis, sensing performance, and mechanism Study, Adv. Funct. Mater. 33 (2023) 2304718, https://doi.org/10.1002/adfm.202304718.
[136] K. Großmann, S. Wicker, U. Weimar, N. Barsan, Impact of Pt additives on the surface reactions between SnO_2, water vapour, CO and H_2; an operando investigation, Phys. Chem. Chem. Phys. 15 (2013) 19151–19158, https://doi.org/10.1039/C3CP52782D.
[137] D. Zhang, J. Tong, B. Xia, Humidity-sensing properties of chemically reduced graphene oxide/polymer nanocomposite film sensor based on layer-by-layer nano self-assembly, Sensor. Actuator. B Chem. 197 (2014) 66–72, https://doi.org/10.1016/j.snb.2014.02.078.
[138] H. Bi, K. Yin, X. Xie, J. Ji, S. Wan, L. Sun, M. Terrones, M.S. Dresselhaus, Ultrahigh humidity sensitivity of graphene oxide, Sci. Rep. 3 (2013) 2714, https://doi.org/10.1038/srep02714.
[139] Y. Wang, Y. Zhou, G. Xie, J. Li, Y. Wang, X. Liu, Z. Zang, Dual resistance and impedance investigation: ultrasensitive and stable humidity detection of Molybdenum disulfide nanosheet-polyethylene oxide hybrids, ACS Appl. Mater. Interfaces 13 (2021) 25250–25259, https://doi.org/10.1021/acsami.1c02119.
[140] A. Ricci, F. Martelli, R. Razzano, D. Cassi, C. Lazzi, E. Neviani, V. Bernini, Service temperature preservation approach for food safety: microbiological evaluation of ready meals, Food Control 115 (2020) 107297, https://doi.org/10.1016/j.foodcont.2020.107297.
[141] D. Leng, H. Zhang, C. Tian, H. Xu, Low temperature preservation developed for special foods in East Asia: a review, J. Food Process. Preserv. 46 (2022) e16176, https://doi.org/10.1111/jfpp.16176.
[142] L. Li, Z. Li, R. Zhong, Z. Du, Z. Luan, S. Xi, X. Zhang, Direct H_2S, HS^- and pH measurements of high-temperature hydrothermal vent fluids with *in situ* Raman spectroscopy, Geophys. Res. Lett. 50 (2023), https://doi.org/10.1029/2023GL103195 e2023GL103195.
[143] V. Preston, G. Flaspohler, J. Kapit, W. Pardis, S. Youngs, D.E. Martocello, N. Roy, P.R. Girguis, S.D. Wankel, A.P.M. Michel, Discovering hydrothermalism from Afar: *in situ* methane instrumentation and change-point detection for decision-making, Front. Earth Sci. 10 (2022) 984355, https://doi.org/10.3389/feart.2022.984355.
[144] B.W. Beckley, C.A. Motil, I.M. Henry, I.S. Chi, M.D. Sprouse, Glenn Extreme Environments Rig (GEER) facility users guide. Planetary Science Technology Symposium: Cleveland, OH, USA, 2024. October 22-24, 2024; NASA Technical Reports Server, Document ID 20240012869, https://ntrs.nasa.gov/citations/20240012869. (Accessed 6 July 2026).
[145] F.A.A. Nugroho, I. Darmadi, L. Cusinato, A. Susarrey-Arce, H. Schreuders, L. J. Bannenberg, A.B. da Silva Fanta, S. Kadkhodazadeh, J.B. Wagner, T. J. Antosiewicz, A. Hellman, V.P. Zhdanov, B. Dam, C. Langhammer, Metal–polymer hybrid nanomaterials for plasmonic ultrafast hydrogen detection, Nat. Mater. 18 (2019) 489–495, https://doi.org/10.1038/s41563-019-0325-4.
[146] M.-S. Jo, K.-H. Kim, J.-S. Lee, S.-H. Kim, J.-Y. Yoo, K.-W. Choi, B.-J. Kim, D.-S. Kwon, I. Yoo, J.-S. Yang, M.-K. Chung, S.-Y. Park, M.-H. Seo, J.-B. Yoon, Ultrafast (~0.6 s), robust, and highly linear hydrogen detection up to 10% using fully suspended pure Pd nanowire, ACS Nano 17 (2023) 23649–23658, https://doi.org/10.1021/acsnano.3c06806.
[147] R. Yang, Z. Yuan, C. Jiang, X. Zhang, Z. Qiao, J. Zhang, J. Liang, S. Wang, Z. Duan, Y. Wu, W. Li, Y. Jiang, H. Tai, Ultrafast hydrogen detection System using vertical thermal conduction structure and neural network prediction Algorithm based on sensor response process, ACS Sens. 10 (2025) 2181–2190, https://doi.org/10.1021/acssensors.4c03487.
[148] T. Huang, Z. Yuan, D. Ma, R. Yang, C. Shan, S. Wang, Z. Duan, Y. Wu, Y. Jiang, H. Tai, Ultrafast (0.3 s) integrated hydrogen leakage sensor system empowered by concentration prediction algorithm, Chem. Eng. J. 520 (2025) 166395, https://doi.org/10.1016/j.cej.2025.166395.
[149] B.W. Holleboom, S.W. Hawes, E.L. Ker, Poisoning of Zirconia exhaust oxygen sensors by Silica, SAE International (1986).
[150] Z. Jin, J. Zhao, L. Liu, F. Liu, Z. Wang, F. Wang, J. Liu, Y. Mou, L. Wu, X. Wu, Humidity-independent gas sensors in the detection of hydrogen sulfide based on

Nd_2O_3-loaded In_2O_3 porous nanorods, Sensor. Actuator. B Chem. 403 (2024) 135237, https://doi.org/10.1016/j.snb.2023.135237.
[151] A.I. Abdulagatov, Y. Yan, J.R. Cooper, Y. Zhang, Z.M. Gibbs, A.S. Cavanagh, R. G. Yang, Y.C. Lee, S.M. George, Al_2O_3 and TiO_2 atomic layer deposition on copper for water corrosion resistance, ACS Appl. Mater. Interfaces 3 (2011) 4593–4601, https://doi.org/10.1021/am2009579.
[152] E.L.W. Gardner, J.W. Gardner, F. Udrea, Micromachined thermal gas Sensors—A review, Sensors 23 (2023), https://doi.org/10.3390/s23020681.
[153] V. Chawla, M. Ruoho, M. Weber, A.A. Chaaya, A.A. Taylor, C. Charmette, P. Miele, M. Bechelany, J. Michler, I. Utke, Fracture mechanics and oxygen gas barrier properties of Al_2O_3/ZnO nanolaminates on PET deposited by atomic layer deposition, Nanomaterials 9 (2019), https://doi.org/10.3390/nano9010088.
[154] M. Putkonen, P. Sippola, L. Svärd, T. Sajavaara, J. Vartiainen, I. Buchanan, U. Forsström, P. Simell, T. Tammelin, Low-Temperature Atomic Layer Deposition of SiO_2/Al_2O_3 Multilayer Structures Constructed on self-standing Films of Cellulose Nanofibrils, 376, 2018 20170037, https://doi.org/10.1098/rsta.2017.0037.
[155] M. Vilaseca, J. Coronas, A. Cirera, A. Cornet, J.R. Morante, J. Santamaría, Use of zeolite films to improve the selectivity of reactive gas sensors, Catal. Today 82 (2003) 179–185, https://doi.org/10.1016/S0920-5861(03)00230-X.
[156] K. Sahner, D. Schönauer, P. Kuchinke, R. Moos, Zeolite cover layer for selectivity enhancement of p-type semiconducting hydrocarbon sensors, Sensor. Actuator. B Chem. 133 (2008) 502–508, https://doi.org/10.1016/j.snb.2008.03.014.
[157] J. Zhang, W. Cheng, H. Wang, L. Zhang, X. Li, H. Ma, J. Pang, Q. Tan, Langasite-based SAW high-temperature vibration sensor with temperature decoupling, Sci. China Technol. Sci. 67 (2024) 1946–1956, https://doi.org/10.1007/s11431-023-2563-4.
[158] H. Zhang, D. Mu, Z. Zhang, J. Zhang, J. Sun, H. Jin, Surface acoustic wave sensors for wireless temperature measurements above 1200 degree celsius, Sensors 24 (2024), https://doi.org/10.3390/s24154945.
[159] V.R. Naganaboina, M. Anandkumar, A.S. Deshpande, S.G. Singh, Single-phase high-entropy oxide-based chemiresistor: toward selective and sensitive detection of methane gas for real-time applications, Sensor. Actuator. B Chem. 357 (2022) 131426, https://doi.org/10.1016/j.snb.2022.131426.
[160] X. Li, X. Chang, X. Liu, J. Zhang, High-entropy oxide $(FeCoNiCrMn)_3O_4$ for room-temperature NO_2 sensors, Appl. Phys. Lett. 124 (2024), https://doi.org/10.1063/5.0191206.
[161] H.G. Yang, C.H. Sun, S.Z. Qiao, J. Zou, G. Liu, S.C. Smith, H.M. Cheng, G.Q. Lu, Anatase TiO_2 single crystals with a large percentage of reactive facets, Nature 453 (2008) 638–641, https://doi.org/10.1038/nature06964.
[162] X. Han, Q. Kuang, M. Jin, Z. Xie, L. Zheng, Synthesis of Titania nanosheets with a high percentage of exposed (001) facets and related photocatalytic properties, J. Am. Chem. Soc. 131 (2009) 3152–3153, https://doi.org/10.1021/ja8092373.
[163] M. Mao, J. Wei, B. Li, L. Li, X. Huang, J. Zhang, Scalable robust photothermal superhydrophobic coatings for efficient anti-icing and de-icing in simulated/real environments, Nat. Commun. 15 (2024) 9610, https://doi.org/10.1038/s41467-024-54058-8.
[164] A. Rescalli, D. Marzorati, S. Gelosa, F. Cellesi, P. Cerveri, Temperature modulation of MOS sensors for enhanced detection of volatile organic compounds, Chemosensors 11 (2023), https://doi.org/10.3390/chemosensors11090501.
[165] F. Sun, R. Sun, J. Yan, Cross-Domain active learning for electronic nose drift compensation, Micromachines 13 (2022), https://doi.org/10.3390/mi13081260.
[166] H. Se, K. Song, C. Sun, J. Jiang, H. Liu, B. Wang, X. Wang, W. Zhang, J. Liu, Online drift compensation framework based on active learning for gas classification and concentration prediction, Sensor. Actuator. B Chem. 398 (2024) 134716, https://doi.org/10.1016/j.snb.2023.134716.
[167] J. Li, G. Xie, X. Zhao, X. Luo, C. Chen, Y. Su, A self-powered wearable uric acid sensor for prolonged monitoring and intervene of hyperuricemia, Chem. Eng. J. 530 (2026) 173622, https://doi.org/10.1016/j.cej.2026.173622.
[168] W. Li, X. Li, X. Xiao, F. Manshaii, X. Luo, G. Chen, W. Li, G. Xie, H. Tai, Y. Jiang, Y. Su, J. Chen, A multimodal sensory textile using programmable ferroelectric nanocomposites, Adv. Mater. 37 (2025) e07169, https://doi.org/10.1002/adma.202507169.
[169] X. Luo, B. Liu, W. Li, B. Li, H. Yuan, Y. Su, Triple-enhanced sensory textiles for self-powered infrared detection, Nano Energy 145 (2025) 111438, https://doi.org/10.1016/j.nanoen.2025.111438.
[170] Y. Gong, C. Bao, Z. He, Y. Jian, X. Wang, H. Huang, X. Song, A review on gas pipeline leak detection: Acoustic-Based, OGI-Based, and multimodal fusion methods, Information 16 (2025), https://doi.org/10.3390/info16090731.
[171] S.G. Ramaraj, A. Alrebh, D. Elamaran, H. Zhou, K. Huang, M. Almansoori, H. Yamahara, H. Tabata, Surface acoustic wave gas sensors: recent developments and their role in sensing technology, Mater. Sci. Eng., B 317 (2025) 118157, https://doi.org/10.1016/j.mseb.2025.118157.
[172] J. Devkota, K.-J. Kim, P.R. Ohodnicki, J.T. Culp, D.W. Greve, J.W. Lekse, Zeolitic imidazolate framework-coated acoustic sensors for room temperature detection of carbon dioxide and methane, Nanoscale 10 (2018) 8075–8087, https://doi.org/10.1039/C7NR09536H.
[173] L. Feng, Y. Liu, Y. Wang, H. Zhou, Z. Lu, T. Li, Ultra-compact dual-channel integrated CO_2 infrared gas sensor, Microsyst. Nanoeng. 10 (2024) 151, https://doi.org/10.1038/s41378-024-00782-6.
[174] D. Li, H. Zhou, Z. Ren, C. Lee, Advances in MEMS, optical MEMS, and nanophotonics technologies for volatile organic compound detection and applications, Small Sci. 5 (2025) 2400250, https://doi.org/10.1002/smsc.202400250.
[175] I.C. Weber, A.T. Güntner, Catalytic filters for metal oxide gas sensors, Sensor. Actuator. B Chem. 356 (2022) 131346, https://doi.org/10.1016/j.snb.2021.131346.
[176] M. Xu, W. Tian, Y. Lin, Y. Xu, J. Tao, Development of a compact NDIR CO_2 gas sensor for a portable gas analyzer, Micromachines 15 (2024), https://doi.org/10.3390/mi15101203.
[177] Z. Ma, G. Luo, K. Qin, N. Wang, W. Niu, Online sensor drift compensation for E-Nose systems using domain adaptation and extreme learning machine, Sensors 18 (2018), https://doi.org/10.3390/s18030742.
[178] A. Rudnitskaya, Calibration update and drift correction for electronic noses and tongues, Front. Chem. 6 (2018), https://doi.org/10.3389/fchem.2018.00433.
[179] R. Huerta, T. Mosqueiro, J. Fonollosa, N.F. Rulkov, I. Rodriguez-Lujan, Online decorrelation of humidity and temperature in chemical sensors for continuous monitoring, Chemometr. Intell. Lab. Syst. 157 (2016) 169–176, https://doi.org/10.1016/j.chemolab.2016.07.004.